Systematic analysis of single heavy baryons Λ_Q, Σ_Q and Ω_Q

Guo-Liang Yu[1],* Zhen-Yu Li[2], Zhi-Gang Wang[1],† Lu Jie[1], and Yan Meng[1]

[1] *Department of Mathematics and Physics, North China Electric Power University, Baoding 071003, People's Republic of China*

[2] *School of Physics and Electronic Science, Guizhou Education University, Guiyang 550018, People's Republic of China*

(Dated: April 4, 2023)

Motivated by great progresses in experiments in searching for the heavy baryons, we systematically analyze the mass spectra and root mean square radius of single heavy baryons Λ_Q, Σ_Q and Ω_Q. The calculations of the mass spectra are carried out in the frame work of relativized quark model, where the baryon is regarded as a three-body system of quarks. Our results show that the mass of single heavy baryon with λ-mode is lower than those of the ρ-mode and λ-ρ mixing mode, which indicates that the lowest state is dominated by the λ-mode. Basing on this research, we systematically calculate the mass spectra and the root mean square radius of the baryons with λ excited mode. With these predicated mass spectra, the Regge trajectories in the (J,M^2) plane are constructed, and the slopes, intercepts of the Regge trajectories are obtained by linear fitting. It is found that all available experimental data are well reproduced by model predictions and fit nicely to the constructed Regge trajectories.

PACS numbers: 13.25.Ft; 14.40.Lb

1 Introduction

In the field of heavy baryon physics, scientists have made great progresses in experiments as well as in theories, which makes the mass spectra of heavy baryon families become more and more abundant. In the past few decades, almost all of the $1S$ single heavy baryons have been well established and some of the $1P$ states $\Lambda_c(2595)$[1], $\Lambda_c(2625)$[2], $\Lambda_b(5912)$ and $\Lambda_b(5920)$[3, 4] have also been well observed in experiments and been confirmed in theory[5, 6]. Besides these states, many other single heavy baryons have also been discovered by Belle, BABAR, CLEO and LHCb, such as $\Lambda_c(2765)$[7], $\Lambda_c(2940)$[8–10], $\Lambda_b(6072)$[11], $\Lambda_b(6146)$[12], $\Lambda_b(6152)$[12], $\Sigma_c(2800)$[13], $\Sigma_b(6097)$[14], $\Omega_c(3000)$, $\Omega_c(3050)$, $\Omega_c(3065)$, $\Omega_c(3090)$, $\Omega_c(3119)$[16], $\Omega_b(6330)$, $\Omega_b(6316)$, $\Omega_b(6350)$ and $\Omega_b(6340)$[15]. Some of these baryons may belong to the low-lying S- or P-wave states, while some of them can be assigned to D-wave baryons and all of these assignments needs further confirmation in more ways. In order to identify their quantum numbers and assign each baryon a suitable position in the mass spectra, it is necessary to

*Electronic address: yuguoliang2011@163.com
†Electronic address: zgwang@aliyun.com

systematically investigate single heavy baryon spectroscopy.

In the past decades, the single heavy baryons have been extensively investigated by many theoretical methods/models, including various quark model[17–44], the heavy hadron chiral perturbation theory[45–50], lattice QCD[51–54], light cone QCD sum rules[55–62], QCD sum rules[63–82] and relativistic flux tube model[83]. To our knowledge, only Ref.[19] focused on the mass spectra of the heavy baryons from ground states to the high excited states systematically in the quark-diquark picture. In this literature, heavy baryons are considered in the heavy-quark-light-diquark approximation, which can simplify the complicated relativistic three-body problem. Under this quark-diquark picture, the initial three-body problem is reduced to two-step two-body calculations. Another important work was carried out by Roberts and Pervin[20]. With the non-relativized quark model, they studied various excited states of single heavy baryons by solving three quark systems explicitly. On the other hand, a Gaussian expansion method(GEM) was introduced in the non-relativized quark model to solve the three-quark system in Ref.[21]. In the calculations of the matrix elements of the Hamiltonian of three-body system, particularly when complicated interactions are employed, integrations over all of the radial and angular coordinates become laborious even with GEM. In Ref.[21], they developed an infinitesimally-shifted Gaussian(ISG) basis function to simplify this process.

In this work, we extend the method of ISG basis function to the relativized quark model to study the mass spectra of the single heavy baryons. The relativized quark model was first developed by Godfrey and Isgur to study the mass spectra of mesons[17], and later was extended by Capstick and Isgur to investigate baryon spectra[18]. Recently, this quark model has also been used to investigate the mass of tetraquark states[84–86]. It was found that GEM is one of the best method for three and four body bound states[21], which can help us to obtain precise energy eigenvalues of excited states. Especially, taking ISG function as the basis function has the advantage of simplifying the calculation of matrix elements[21]. The first goal of our present work is to calculate the mass spectra and root mean square radius of the excited heavy baryons up to rather high orbital and radial excitations. With these results, we will construct the heavy baryon Regge trajectories in the (J,M^2) planes and determine their Regge slopes and intercepts.

The paper is organized as follows. In Section II, we present the the relativized quark model of heavy baryons based on the method of ISG basis functions. With this method, we systematically investigate the mass spectra and root mean square radius of single heavy baryons Λ_Q, Σ_Q and Ω_Q. In Sec III the heavy baryon Regge trajectories in the $(J,\, M^2)$ plane are constructed with the predicted mass spectra, and slopes, intercepts of parent and daughter trajectories are also obtained by linear fitting. And Sec IV is reserved for our conclusions.

2 Phenomenological method adopted in this work

2.1 The Jacobi coordinate and relativized quark model

In this work, the single heavy baryon is regarded as a three-body system which has two light quarks(u, d or s quarks) and one heavy quark(c or b quark) inside. In order to express internal motions of the quarks in this three-body system, we commonly introduce three sets of Jacobi coordinates as in Fig.1. Each set of Jacobi coordinate is called a channel(c) which is defined as,

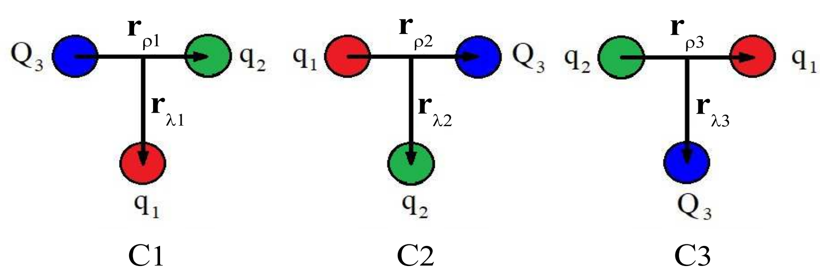

FIG. 1: Jacobi coordinates for the three body system.

$$\boldsymbol{r}_\lambda = \boldsymbol{r}_k - \frac{m_i \boldsymbol{r}_i + m_j \boldsymbol{r}_j}{m_i + m_j} \tag{1}$$

$$\boldsymbol{r}_\rho = \boldsymbol{r}_i - \boldsymbol{r}_j \tag{2}$$

where assignments of (i,j,k) are given in Table I. The Jacobi coordinate of $c = 3$ can be expressed in

Channel	i	j	k
$c = 1$	2	3	1
$c = 2$	3	1	2
$c = 3$	1	2	3

TABLE I: The quark assignments (i,j,k) for the Jacobi coordinates

terms of the coordinate $c = 1$ or $c = 2$,

$$\boldsymbol{r}_{\rho_3} = \alpha^r_{31(32)} \boldsymbol{r}_{\rho_{1(2)}} + \beta^r_{31(32)} \boldsymbol{r}_{\lambda_{1(2)}} \tag{3}$$

$$\boldsymbol{r}_{\lambda_3} = \gamma^r_{31(32)} \boldsymbol{r}_{\rho_{1(2)}} + \delta^r_{31(32)} \boldsymbol{r}_{\lambda 1(2)} \tag{4}$$

where the transforming coefficients for $c : 3 \to 1$ and $3 \to 2$ are,

$$\alpha^r_{31} = -\frac{m_3}{m_2+m_3}, \beta^r_{31} = 1, \gamma^r_{31} = -\frac{m_2(m_1+m_2+m_3)}{(m_1+m_2)(m_2+m_3)}, \delta^r_{31} = -\frac{m_1}{m_1+m_2},$$

$$\alpha^r_{32} = -\frac{m_3}{m_1+m_3}, \beta^r_{32} = -1, \gamma^r_{32} = \frac{m_1(m_1+m_2+m_3)}{(m_1+m_2)(m_1+m_3)}, \delta^r_{32} = -\frac{m_2}{m_1+m_2}.$$

In the following, we give a brief introduction to the Hamiltonian of relativized quark model. The relativistic Hamiltonian for a three-body system can be written as[17, 18],

$$\widehat{H} = \sum_{i=1}^{3} (p_i^2 + m_i^2)^{1/2} + \sum_{i<j} \widetilde{H}^{\mathrm{conf}}_{ij} + \sum_{i<j} \widetilde{H}^{\mathrm{hyp}}_{ij} + \sum_{i<j} \widetilde{H}^{\mathrm{so}}_{ij} \tag{5}$$

where the first term is the relativistic kinetic energy term, $\widetilde{H}^{\rm conf}$ is the spin-independent potential which contains a linear confining potential $\widetilde{S}(r_{ij})$ and the one-gluon exchange potential $G'(r_{ij})$,

$$\widetilde{H}^{\rm conf}_{ij} = \widetilde{S}(r_{ij}) + G'(r_{ij}) \tag{6}$$

with

$$\widetilde{S}(r_{ij}) = -\frac{3}{4}\boldsymbol{F}_i\cdot\boldsymbol{F}_j\Big[br_{ij}\big[\frac{e^{-\sigma_{ij}^2 r_{ij}^2}}{\sqrt{\pi}\sigma_{ij}r_{ij}} + \big(1+\frac{1}{2\sigma_{ij}^2 r_{ij}^2}\big)\frac{2}{\sqrt{\pi}}\int_0^{\sigma_{ij}r_{ij}} e^{-x^2}dx\big] + c\Big] \tag{7}$$

$$\sigma_{ij} = \sqrt{s^2\Big[\frac{2m_i m_j}{m_i+m_j}\Big]^2 + \sigma_0^2\Big[\frac{1}{2}\big(\frac{4m_i m_j}{(m_i+m_j)^2}\big)^4 + \frac{1}{2}\Big]} \tag{8}$$

The $\boldsymbol{F}_i\cdot\boldsymbol{F}_j$ stands for the color matrix and F_n reads

$$F_n = \begin{cases} \frac{\lambda_n}{2} & \text{for quarks,} \\ -\frac{\lambda_n^*}{2} & \text{for antiquarks} \end{cases} \tag{9}$$

with $n = 1, 2\cdots 8$. It should be noticed that the one-gluon exchange potential $G'(r_{ij})$ is achieved by introducing momentum-dependent factors,

$$G'(r_{ij}) = \Big(1+\frac{p_{ij}^2}{E_iE_j}\Big)^{\frac{1}{2}}\widetilde{G}(r_{ij})\Big(1+\frac{p_{ij}^2}{E_iE_j}\Big)^{\frac{1}{2}} \tag{10}$$

with

$$\widetilde{G}(r_{ij}) = \boldsymbol{F}_i\cdot\boldsymbol{F}_j\sum_{k=1}^{3}\frac{2\alpha_k}{3\sqrt{\pi}r_{ij}}\int_0^{\tau_k r_{ij}} e^{-x^2}dx \tag{11}$$

and $\tau_k = \frac{1}{\sqrt{\frac{1}{\sigma_{ij}^2}+\frac{1}{\gamma_k^2}}}$.

In, Eq.(5), $\widetilde{H}^{\rm hyp}$ is the color-hyperfine interaction which includes tensor interaction and the contact interaction,

$$\widetilde{H}^{\rm hyp}_{ij} = \widetilde{H}^{\rm tensor}_{ij} + \widetilde{H}^{\rm c}_{ij} \tag{12}$$

with

$$\widetilde{H}^{\rm tensor}_{ij} = -\Big(\frac{\mathbf{S}_i\cdot\mathbf{r}_{ij}\mathbf{S}_j\cdot\mathbf{r}_{ij}/r_{ij}^2 - \frac{1}{3}\mathbf{S}_i\cdot\mathbf{S}_j}{m_i m_j}\Big)\times\Big(\frac{\partial^2}{\partial r_{ij}^2} - \frac{1}{r_{ij}}\frac{\partial}{\partial r_{ij}}\Big)\widetilde{G}^{\rm t}_{ij}, \tag{13}$$

$$\widetilde{H}^{\rm c}_{ij} = \frac{2\mathbf{S}_i\cdot\mathbf{S}_j}{3m_i m_j}\bigtriangledown^2\widetilde{G}^{\rm c}_{ij} \tag{14}$$

For the spin-orbit interaction, it can be divided into two parts which can be written as,

$$\widetilde{H}^{\rm so}_{ij} = \widetilde{H}^{\rm so(v)}_{ij} + \widetilde{H}^{\rm so(s)}_{ij}, \tag{15}$$

with

$$\widetilde{H}^{\rm so(v)}_{ij} = \frac{\mathbf{S}_i\cdot\mathbf{L}_{ij}}{2m_i^2 r_{ij}}\frac{\partial \widetilde{G}^{\rm so(v)}_{ii}}{\partial r_{ij}} + \frac{\mathbf{S}_j\cdot\mathbf{L}_{ij}}{2m_j^2 r_{ij}}\frac{\partial \widetilde{G}^{\rm so(v)}_{jj}}{\partial r_{ij}} + \frac{(\mathbf{S}_i+\mathbf{S}_j)\cdot\mathbf{L}_{ij}}{m_i m_j r_{ij}}\frac{1}{r_{ij}}\frac{\partial \widetilde{G}^{\rm so(v)}_{ij}}{\partial r_{ij}} \tag{16}$$

and

$$\widetilde{H}^{\rm so(s)}_{ij} = -\frac{\mathbf{S}_i\cdot\mathbf{L}_{ij}}{2m_i^2 r_{ij}}\frac{\partial \widetilde{S}^{\rm so(s)}_{ii}}{\partial r_{ij}} - \frac{\mathbf{S}_j\cdot\mathbf{L}_{ij}}{2m_j^2 r_{ij}}\frac{\partial \widetilde{S}^{\rm so(s)}_{jj}}{\partial r_{ij}} \tag{17}$$

In Eqs.(13),(14),(16) and (17), $\widetilde{G}^{\rm t}_{ij}$, $\widetilde{G}^{\rm c}_{ij}$, $\widetilde{G}^{\rm so(v)}_{ij}$ and $\widetilde{S}^{\rm so(s)}_{ii}$ are achieved from $\widetilde{G}(r_{ij})$ and $\widetilde{S}(r_{ij})$ by introducing momentum-dependent factors,

$$G^{\rm t}_{ij} = \left(\frac{m_i m_j}{E_i E_j}\right)^{\frac{1}{2}+\epsilon_{\rm t}} \widetilde{G}(r_{ij}) \left(\frac{m_i m_j}{E_i E_j}\right)^{\frac{1}{2}+\epsilon_{\rm t}} \tag{18}$$

$$G^{\rm c}_{ij} = \left(\frac{m_i m_j}{E_i E_j}\right)^{\frac{1}{2}+\epsilon_{\rm c}} \widetilde{G}(r_{ij}) \left(\frac{m_i m_j}{E_i E_j}\right)^{\frac{1}{2}+\epsilon_{\rm c}} \tag{19}$$

$$G^{\rm so(v)}_{ij} = \left(\frac{m_i m_j}{E_i E_j}\right)^{\frac{1}{2}+\epsilon_{\rm so(v)}} \widetilde{G}(r_{ij}) \left(\frac{m_i m_j}{E_i E_j}\right)^{\frac{1}{2}+\epsilon_{\rm so(v)}} \tag{20}$$

$$\widetilde{S}^{\rm so(s)}_{ii} = \left(\frac{m_i^2}{E_i^2}\right)^{\frac{1}{2}+\epsilon_{\rm so(s)}} \widetilde{S}(r_{ij}) \left(\frac{m_i^2}{E_i^2}\right)^{\frac{1}{2}+\epsilon_{\rm so(s)}} \tag{21}$$

with $E_i = \sqrt{m_i^2 + p_{ij}^2}$, and $\epsilon_{\rm t}$, $\epsilon_{\rm c}$, $\epsilon_{\rm so(v)}$ and $\epsilon_{\rm so(s)}$ are free parameters that are discussed in Table II. The p_{ij} is the magnitude of the momentum of either of the quarks in the ij center-of-mass frame and these relative momentums p_{23}, p_{13} and p_{12} correspond to p_{ρ_1}, p_{ρ_2} and p_{ρ_3} in three channels.

2.2 Wave function of single heavy baryon

In quark model scheme, the full wave function for a definite baryon is built from a linear superposition of the channel wave function, which can be written as,

$$\Psi^{JM}_{full} = \sum_{c\alpha} C_{c,\alpha}\Psi^c_{JM}(\boldsymbol{r}_{\rho_c}, \boldsymbol{r}_{\lambda_c}) \tag{22}$$

where the index α denotes n_ρ,n_λ,l_ρ,l_λ,L,s,j, and c denotes the Jacobi coordinate channel with $c = 1, 2, 3$ as illustrated in Fig.1. $\Psi^c_{JM}(\boldsymbol{r}_{\rho_c}, \boldsymbol{r}_{\lambda_c})$ is the wave function for channel c and it is described in terms of antisymmetric color-singlet wave function $\phi_{\rm color}$, multiplying flavor $\phi_{\rm flavor}$, spin and space wave function ψ^c_{JM}

$$\Psi^c_{JM}(\boldsymbol{r}_{\rho_c}, \boldsymbol{r}_{\lambda_c}) = \phi_{\rm color}\otimes\phi_{\rm flavor}\otimes\psi^c_{JM} \tag{23}$$

with

$$\phi_{\rm color} = \frac{1}{\sqrt{6}}\big(rgb - rbg + gbr - grb + brg - bgr\big), \tag{24}$$

$$\psi^c_{JM} = \Big[\big[[\chi_{1/2}(q)\chi_{1/2}(q)]_{s,m_s}\Phi^c_{l_\rho,l_\lambda,L}\big]_{j,m_j}\chi_{1/2}(Q)\Big]_{JM}, \tag{25}$$

where r, g, b are the color of the quark and $\chi_{1/2}$ is the spin wave function. Within the flavor SU(3) subgroups, the single heavy baryons belong either to a sextet(6_F) of flavor symmetric states, or an antitriplet($\overline{3}_F$) of flavor antisymmetric states. For the Σ_Q and Ω_Q baryons, they belong to flavor-symmetric sextet ϕ_{6_F}, while Λ_Q baryon is flavor-antisymmetric antitriplet $\phi_{\overline{3}_F}$. In Eq.(25), $\Phi^c_{l_\rho,l_\lambda,L}$ is the spatial wave function which is constructed from the wave functions of the two Jacobi coordinates ρ and λ, and takes the form

$$\Phi^c_{l_\rho,l_\lambda,L} = \Big[\phi_{l_\rho m_{l_\rho}}(\boldsymbol{r}_{\rho_c})\phi_{l_\lambda m_{l_\lambda}}(\boldsymbol{r}_{\lambda_c})\Big]_L \quad c=1,2,3 \tag{26}$$

In this work, the spatial wave function of a three-body system is expanded in terms of a set of Gaussian basis functions. Thus, $\phi_{l_\rho m_{l_\rho}}(\boldsymbol{r}_{\rho_c})$ and $\phi_{l_\lambda m_{l_\lambda}}(\boldsymbol{r}_{\lambda_c})$ in Eq.(26) are written as,

$$\phi_{n_\rho l_\rho m_{l_\rho}}(\boldsymbol{r}_{\rho_c}) = N_{n_\rho l_\rho} r_{\rho_c}^{l_\rho} e^{-\nu_{n_\rho} r^2_{\rho_c}} Y_{l_\rho m_{l_\rho}}(\hat{\boldsymbol{r}}_{\rho_c}) \tag{27}$$

$$\phi_{n_\lambda l_\lambda m_{l_\lambda}}(\boldsymbol{r}_{\lambda_c}) = N_{n_\lambda l_\lambda} r_{\lambda_c}^{l_\lambda} e^{-\nu_{n_\lambda} r^2_{\lambda_c}} Y_{l_\lambda m_{l_\lambda}}(\hat{\boldsymbol{r}}_{\lambda_c}) \tag{28}$$

with

$$N_{n_\rho l_\rho} = \sqrt{\frac{2^{l_\rho+2}(2\nu_{n_\rho})^{l_\rho+3/2}}{\sqrt{\pi}(2l_\rho+1)!!}} \tag{29}$$

$$N_{n_\lambda l_\lambda} = \sqrt{\frac{2^{l_\lambda+2}(2\nu_{n_\lambda})^{l_\lambda+3/2}}{\sqrt{\pi}(2l_\lambda+1)!!}} \tag{30}$$

$$\nu_{n_\rho} = \frac{1}{r^2_{n_\rho}}, \quad r_{n_\rho} = r_a\Big[\frac{r_{amax}}{r_a}\Big]^{\frac{n-1}{n_{max}-1}} \quad (n=1,\cdots,n_{max}) \tag{31}$$

$$\nu_{n_\lambda} = \frac{1}{r^2_{n_\lambda}}, \quad r_{n_\lambda} = r_b\Big[\frac{r_{bmax}}{r_b}\Big]^{\frac{n-1}{n_{max}-1}} \quad (n=1,\cdots,n_{max}) \tag{32}$$

where r_a, r_b, r_{amax} and r_{bmax} are the Gaussian range parameters, which take the values as r_a = r_b=0.18, r_{amax} = r_{bmax}=15. The n_{max} is the maximum number of the Gaussian basis functions which is determined as 10 in Section 3.1. In momentum space, the Gaussian basis functions can be written as,

$$\phi_{n_\rho l_\rho m_{l_\rho}}(\boldsymbol{p}_{\rho_c}) = N'_{n_\rho l_\rho} p_{\rho_c}^{l_\rho} e^{-\frac{p^2_{\rho_c}}{4\nu_{n_\rho}}} Y_{l_\rho m_{l_\rho}}(\hat{\boldsymbol{p}}_{\rho_c}) \tag{33}$$

$$\phi_{n_\lambda l_\lambda m_{l_\lambda}}(\boldsymbol{p}_{\lambda_c}) = N'_{n_\lambda l_\lambda} p_{\lambda_c}^{l_\lambda} e^{-\frac{p^2_{\lambda_c}}{4\nu_{n_\lambda}}} Y_{l_\lambda m_{l_\lambda}}(\hat{\boldsymbol{p}}_{\lambda_c}) \tag{34}$$

with

$$N'_{n_\rho l_\rho} = (-i)^{l_\rho}\sqrt{\frac{2^{l_\rho+2}}{\sqrt{\pi}(2\nu_{n_\rho})^{l_\rho+3/2}(2l_\rho+1)!!}} \tag{35}$$

$$N'_{n_\lambda l_\lambda} = (-i)^{l_\lambda}\sqrt{\frac{2^{l_\lambda+2}}{\sqrt{\pi}(2\nu_{n_\lambda})^{l_\lambda+3/2}(2l_\lambda+1)!!}} \tag{36}$$

In the heavy quark limit, one heavy quark within the heavy baryon system is decoupled from two light quarks. Under this picture, the interactions which depend on the spin of the heavy quark disappear. Thus, two states whose quantum number are $J = j + 1/2$ and $J = j - 1/2$ will be degenerate, where j denotes the light-spin-component. It can be seen from Fig.1 that the picture of Jacobi coordinate channel 3 properly reflects the characteristic of the heavy quark symmetry. As it is shown in Fig.1, the degree of freedom between two light quarks is commonly called the ρ-mode, while the degree between the center of mass of two light quarks and the heavy quark is called the λ-mode. In the SU(3) limit in the light quark sector, the λ- and ρ-modes are mixed. While in the heavy quark limit, it was indicated by Ref.[21] that the excitation energy of the λ-mode is lower than that of the ρ-mode for the P-wave baryon. They drew the conclusion that the lowest state of a P-wave single heavy baryon is dominated by the λ-mode. The first motivation of our present work is to further study the mass spectra of different excitation modes, λ-mode, ρ-mode and λ-ρ mixing mode, with higher orbital excitation. Basing on these above considerations, we perform our calculations in the channel 3 and rewrite the full wave function of a single heavy baryon as,

$$\Psi^{JM}_{full} = \sum_{n_\rho,n_\lambda} C_{n_\rho,n_\lambda}\Psi^3_{JM}(\boldsymbol{r}_{\rho_3},\boldsymbol{r}_{\lambda_3}) \tag{37}$$

2.3 Evaluations of the matrix elements

In the calculations of the Hamiltonian matrix elements of three-body system, particularly when complicated interactions are employed, integrations over all of the radial and angular coordinates become laborious even with Gaussian basis functions. This process can be simplified by introducing the ISG basis functions. For Jacobi coordinates ρ and λ in channel 3, these new sets of basis functions can be written as[87],

$$\phi_{n_\rho l_\rho m_{l_\rho}}(\boldsymbol{r}_\rho) = N_{n_\rho l_\rho}\lim_{\varepsilon\to 0}\frac{1}{(\nu_{n_\rho}\varepsilon)^{l_\rho}}\sum_{k=1}^{k_{max}} C_{l_\rho m_{l_\rho},k}\, e^{-\nu_{n_\rho}(\boldsymbol{r}_\rho-\varepsilon\mathbf{D}_{l_\rho m_{l_\rho},k})^2} \tag{38}$$

$$\phi_{n_\lambda l_\lambda m_{l_\lambda}}(\boldsymbol{r}_\lambda) = N_{n_\lambda l_\lambda}\lim_{\varepsilon\to 0}\frac{1}{(\nu_{n_\lambda}\varepsilon)^{l_\lambda}}\sum_{K=1}^{K_{max}} C_{l_\lambda m_{l_\lambda},K}\, e^{-\nu_{n_\lambda}(\boldsymbol{r}_\lambda-\varepsilon\mathbf{D}_{l_\lambda m_{l_\lambda},K})^2} \tag{39}$$

where ε is the shifted distance of the Gaussian basis. Taking the limit $\varepsilon \to 0$ is to be carried out after the matrix elements have been calculated analytically.

All of the evaluated matrix elements are presented in **Appendixes B.1-B.5**. Finally, the mass spectra can be obtained by solving the generalized eigenvalue problem,

$$\sum_{j=1}^{n_{max}^2} \Big(H_{ij} - EN_{ij}\Big)C_j = 0, \quad (i = 1 - n_{max}^2) \tag{40}$$

Where H_{ij} denotes the matrix element in the total color-flavor-spin-spatial base, E is the eigenvalue, C_j stands for the corresponding eigenvector, and N_{ij} is the overlap matrix elements of the Gaussian functions, which arises from the nonorthogonality of the bases and can be expressed as,

$$\begin{aligned} N_{ij} &\equiv \langle \phi_{n_{\rho_a} l_{\rho_a} m_{l_{\rho_a}}} | \phi_{n_{\rho_b} l_{\rho_b} m_{l_{\rho_b}}} \rangle \times \langle \phi_{n_{\lambda_a} l_{\lambda_a} m_{l_{\lambda_a}}} | \phi_{n_{\lambda_b} l_{\lambda_b} m_{l_{\lambda_b}}} \rangle \\ &= \Big(\frac{2\sqrt{\nu_{n_{\rho_a}} \nu_{n_{\rho_b}}}}{\nu_{n_{\rho_a}} + \nu_{n_{\rho_b}}} \Big)^{l_{\rho_a}+3/2} \times \Big(\frac{2\sqrt{\nu_{n_{\lambda_a}} \nu_{n_{\lambda_b}}}}{\nu_{n_{\lambda_a}} + \nu_{n_{\lambda_b}}} \Big)^{l_{\lambda_a}+3/2} \end{aligned} \tag{41}$$

3 Mass spectra and root mean square radius

3.1 Numerical stabilities and λ-modes

TABLE II: Relevant parameters of the relativized quark model

m_u/m_d(MeV)	m_s(MeV)	m_c(MeV)	m_b(MeV)	α_1	α_2
220	419	1628	4997	0.25	0.15
α_3	γ_1(GeV)	γ_2(GeV)	γ_3(GeV)	b(GeV^2)	c(MeV)
0.20	$\frac{1}{2}$	$\sqrt{10}/2$	$\sqrt{1000}/2$	0.14	-198
σ_0(GeV)	s	$\epsilon_{\rm c}$	$\epsilon_{\rm (so)v}$	$\epsilon_{\rm t}$	$\epsilon_{\rm (so)s}$
1.8	1.55	-0.168	-0.035	0.025	0.055

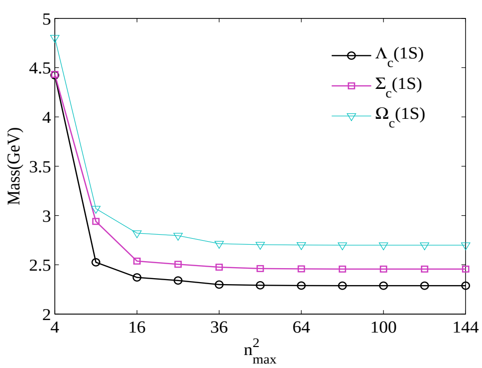

FIG. 2: Convergence of the energy of the lowest Λ_c, Σ_c and Ω_c for increasing the number of bases functions.

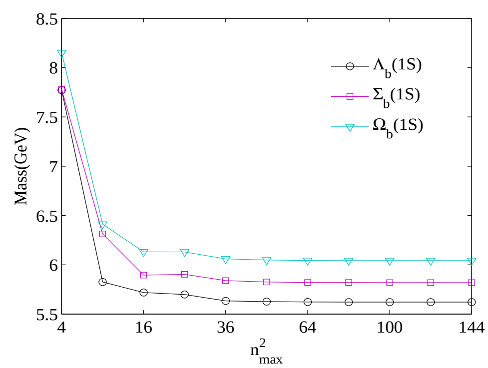

FIG. 3: Convergence of the energy of the lowest Λ_b, Σ_b and Ω_b for increasing the number of bases functions.

Most of the parameters used in this work are taken from the original reference[18] and they are all collected in Table II for convenience. To reproduce the lowest-lying baryon mass spectra, we repair the values of parameters b and c in the line confining potential from 0.18 and -253 to 0.14 and -198. In the relativized quark model, the stability of the numerical results depends strongly on the number of bases. Theoretically, the number of bases should be large enough to guarantee approximate completeness, otherwise the numerical results are not reliable. In order to investigate the convergence and stability of the numerical results, we plot the eigen-energy of the lowest lying $\Lambda_Q(\frac{1}{2}^+)$, $\Sigma_Q(\frac{1}{2}^+)$ and $\Omega_Q(\frac{1}{2}^+)$ baryons in Figs. 2-3. We can see that the eigenvalues decrease with the basis number and converge to a stable value when the $n_{max}^2 = 10^2$. Thus, it is enough for us to obtain the mass spectra with 10^2 Gaussian bases in present work.

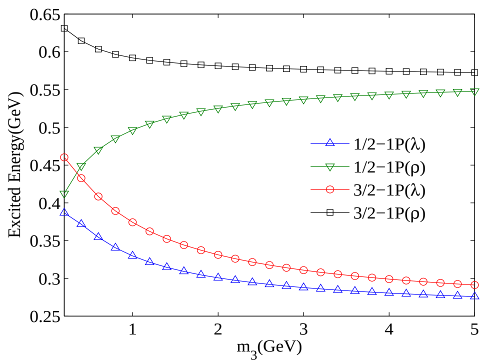

FIG. 4: Heavy quark mass dependence of excited energy of $1P$ $\Lambda_Q(\frac{1}{2}^-,\frac{3}{2}^-)$ with λ mode and ρ mode

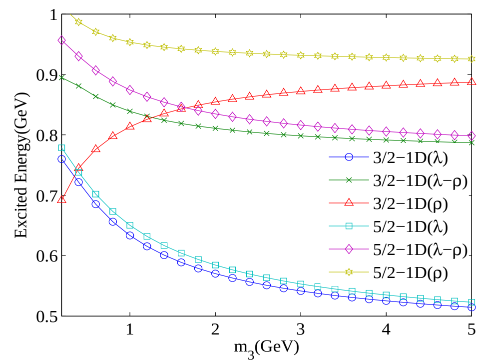

FIG. 5: Heavy quark mass dependence of excited energy of $1D$ $\Lambda_Q(\frac{3}{2}^+,\frac{5}{2}^+)$ with λ mode ,ρ mode and λ-ρ mixing mode

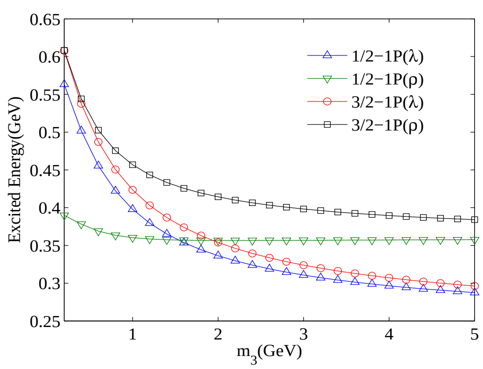

FIG. 6: Heavy quark mass dependence of excited energy of $1P$ $\Sigma_Q(\frac{1}{2}^-,\frac{3}{2}^-)$ with λ mode and ρ mode

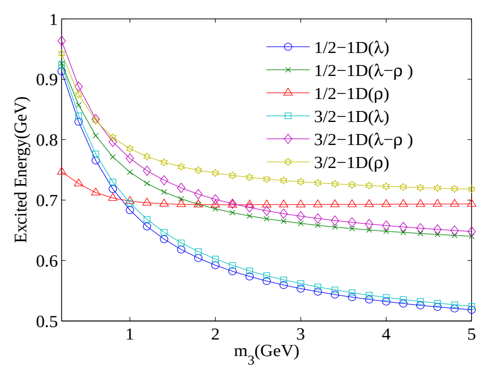

FIG. 7: Heavy quark mass dependence of excited energy of $1D$ $\Sigma_Q(\frac{1}{2}^+,\frac{3}{2}^+)$ with λ mode ,ρ mode and λ-ρ mixing mode

In the scheme of channel 3, the orbital angular momentum between the two light quarks is denoted

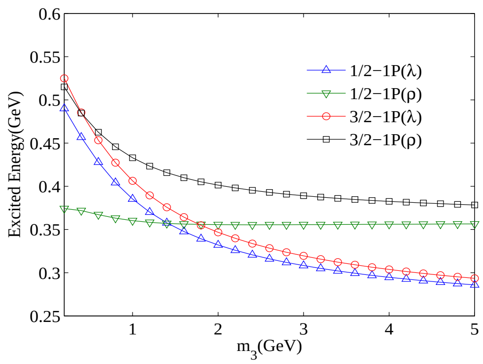

FIG. 8: Heavy quark mass dependence of excited energy of $1P$ $\Omega_Q(\frac{1}{2}^-,\frac{3}{2}^-)$ with λ mode and ρ mode.

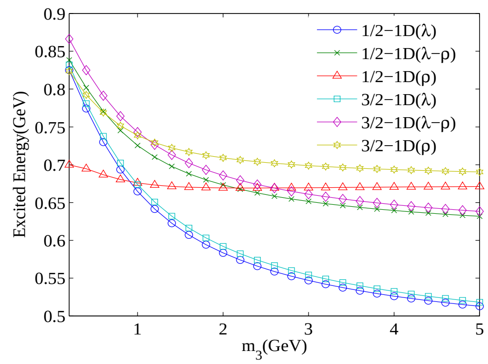

FIG. 9: Heavy quark mass dependence of excited energy of $1D$ $\Omega_Q(\frac{1}{2}^+,\frac{3}{2}^+)$ with λ mode, ρ mode and λ-ρ mixing mode

by l_ρ, while the angular momentum between the light diquarks and the heavy quark is denoted by l_λ. For P-wave baryons, there are two orbital excitation modes λ- and ρ-mode with (l_ρ,l_λ)=(0,1) and (1,0) respectively. While there are three excitation modes for D-wave baryon with (l_ρ,l_λ)=(0,2), (2,0) and (1,1), which are called the λ-mode, ρ-mode and λ-ρ mixing mode, respectively. For higher angular excited states, they are similar with the D-wave baryon, which also have three excitation modes. To investigate the mass spectra of these different excitation modes, we change the heavy quark mass m_Q, from 0.2 GeV to 5.0 GeV and analyze their excitation energies. Figs. 4-9 show the results of Λ_Q, Σ_Q and Ω_Q systems. We can see that as m_Q becomes large, the λ-mode appears lower in excited energy than both the ρ-mode and λ-ρ mixing mode for these baryons. This indicates the lowest state becomes dominated by the λ-mode as m_Q becomes large whether for P- or D-wave baryon. In Figs. 4-5, the λ dominance is seen at about $m_Q = 0.4$ GeV for Λ_Q baryon and this feature appears at $m_Q \geq 1.0$ GeV for D-wave Σ_Q and Ω_Q(see Figs. 7 and 9). For P-wave Σ_Q and Ω_Q systems(see Figs. 6 and 8), although λ and ρ excited modes are separated more slowly, the λ dominance is also seen at about $m_Q \geq 1.6$ GeV.

From these figures, the heavy quark spin symmetry(HQS) is also displayed. For P-wave Λ_Q as an example(see Fig. 4), when m_Q increases from 0.2 GeV to 5.0 GeV, the splitting of the spin-doublet $(\frac{1}{2}^-,\frac{3}{2}^-)$ of λ excitation mode decreases from 80 MeV to 10 MeV. And this behavior is more obvious for P-wave Λ_Q baryon with ρ-mode(see Fig. 4).

3.2 Mass spectra of Λ_Q, Σ_Q and Ω_Q

From these above discussions, we know that each state of the single heavy baryons is dominated and characterized by the λ-mode. Thus, we obtain the mass spectra of the Λ_Q, Σ_Q, and Ω_Q baryons with λ excitation mode. Our predictions for mass spectra and root mean square radius are shown in **Appendix A.1**(Tables III-VIII). In the first two columns of these tables we give the baryon quantum numbers ($l_\rho\ l_\lambda\ L\ s\ j$) and $nL(J^P)$, while in the remaining columns our results, experimental data and the results from other models are shown.

A. Λ_Q states

It can be seen from Tables III-IV, the available experimental data for Λ_Q states are well reproduced by the quark model in present work. There are a few observed states, $\Lambda_c(2765)$, $\Lambda_c(2940)$ and $\Lambda_b(6070)$, whose spin and parity have not been confirmed in the latest PDG[5, 6]. Our prediction for the mass of $2S(\frac{1}{2}^+)$ state is 2.764 GeV, which is very close to the experimental data for $\Lambda_c(2765)$. Thus, it is reasonable to describe $\Lambda_c(2765)$ as a $2S(\frac{1}{2}^+)$ state. In the latest PDG, the spin parity of $\Lambda_c(2940)$ was suggested to be $J^P = \frac{3}{2}^-$, but was not confirmed. Model predictions for $2P(\frac{1}{2}^-)$ and $2P(\frac{3}{2}^-)$ states are 2.988 GeV and 3.013 GeV, respectively. By comparing with the experimental data, the $2P(\frac{1}{2}^-)$ state seems to be a better candidate for $\Lambda_c(2940)$ than $2P(\frac{3}{2}^-)$. The predicted mass for $2P(\frac{1}{2}^-)$ baryon is about 50 MeV higher than the experimental data. This notable exception to this state is also seen in the predictions in Ref.[19]. For $\Lambda_b(6070)$, its quantum numbers were suggested to be $2S(\frac{1}{2}^+)$ in Refs.[76, 88]. Our prediction for this state is 6.041 GeV, which is 29 MeV lighter than the experimental data. Under the uncertainties of the model, this result is still within the realm of validity for model like these.

Besides of these above states, some other low-lying Λ_Q states are also predicted in present work, which have not been observed in experiments. First, it is the $2P$-wave $\Lambda_c(\frac{3}{2}^-)$ state which belongs to a spin-doublet $(\frac{1}{2}^-,\frac{3}{2}^-)$ and its model predicted mass is 3.013 GeV. In addition, there are two Λ_b model states that still remain to be found in experiments. They are the partners of the $2P$-wave doublet $(\frac{1}{2}^-,\frac{3}{2}^-)$ of Λ_c, and their masses are predicted to be 6.238 GeV and 6.249 GeV, respectively.

B. Σ_Q states

The lowest states of S-wave Σ_c and Σ_b baryons with the quantum numbers $J^P = \frac{1}{2}^+$ and $J^P = \frac{3}{2}^+$ have been observed and confirmed in experiments[5]. In Tables V-VI, it can be seen that model predictions for these S-wave Σ_Q baryons also agree well with the experimental data. In addition, quark model predicts two spin doublets $(\frac{1}{2}^-,\frac{3}{2}^-)$, $(\frac{3}{2}^-,\frac{5}{2}^-)$ and a singlet $\frac{1}{2}^-$ for $1P$-wave Σ_Q baryons. The previously observed $\Sigma_c(2800)$ and $\Sigma_b(6097)$ states are good candidates for the P-wave states. We can see from Tables V-VI that predicted masses of these lowest P-wave states are very close to each other and they are all comparable with the experimental data of $\Sigma_c(2800)$ or $\Sigma_b(6097)$. It is shown in Table V that there are two states whose masses are closer to the experimental result of $\Sigma_c(2800)$, namely, the states $1P(\frac{1}{2}^-)_{j=1}$ with a mass 2.809 GeV and $1P(\frac{3}{2}^-)_{j=2}$ with 2.802 GeV. In Table VI, two Σ_b states $1P(\frac{1}{2}^-)_{j=1}$ and $1P(\frac{3}{2}^-)_{j=2}$ have masses 6.107 GeV and 6.104 GeV respectively, both excellently match to the experimental state $\Sigma_b(6097)$. Now, it is difficult for us to confirm the quantum numbers of $\Sigma_c(2800)$ and $\Sigma_b(6097)$ only through the mass spectra. If the strong decay behaviors of these P-wave Σ_Q systems were analyzed, better assignments will be suggested.

It can be seen from Tables V-VI, more efforts are needed in searching for Σ_Q baryons in experiments because many model-predicted states are still missing. Besides of $\Sigma_c(2800)$ and $\Sigma_b(6097)$, the other $1P$ states have good potentials to be observed within the mass spectra predicted in present work. On the other hand, it is shown in Tables V-VI that the splitting between the $1P$ and $2S$ state is about 100 MeV, while the splitting between the five $1P$ states ranges from several to 30 MeV. We hope these information will be helpful in searching for these $2S$ and $1P$ Σ_Q states in future experiments. Finally, the $1D$-wave Σ_Q states are most likely to be observed in forthcoming experiments as well. The predicted masses range from 3.072 GeV to 3.084 GeV for $1D$-wave Σ_c states and from 6.338 GeV to 6.346 GeV for Σ_b ones.

C. Ω_Q states

For Ω_Q systems, there are only three states, the lowest S-wave Ω_c doublet $(\frac{1}{2}^+,\frac{3}{2}^+)$ and $1S$-wave $\Omega_b(\frac{1}{2}^+)$, that have been discovered and confirmed[5]. In Tables VII-VIII, it can be seen that the known Ω_Q states are well reproduced by the quark model. However, the predicted $1S(\frac{3}{2}^+)$ Ω_b state with a mass of 6.069 GeV still remains to be found. In the last few years, several new Ω_c and Ω_b states were observed and they are $\Omega_c(3000)$, $\Omega_c(3050)$, $\Omega_c(3066)$, $\Omega_c(3090)$, $\Omega_c(3119)$[16], $\Omega_b(6316)$, $\Omega_b(6330)$, $\Omega_b(6340)$ and $\Omega_b(6350)$[15]. Model prediction for the Ω_c state of $2S(\frac{1}{2}^+)$ is 3.150 GeV, which is close to $\Omega_c(3119)$. If model uncertainties are considered, $\Omega_c(3119)$ can be interpreted as a $2S(\frac{1}{2}^+)$ state. The other four Ω_c baryons can be assigned as the lowest P-wave states because their measured masses are compatible with model predictions in Table VII. For the $1P$-wave Ω_c doublets $(\frac{1}{2}^-, \frac{3}{2}^-)$ and $(\frac{3}{2}^-, \frac{5}{2}^-)$, it is showed in Table VII that the splitting of these doublets are 17 MeV and 28 MeV, respectively. In comparison with the experimental data, the possible assignments for these four experimental Ω_c states are ($\Omega_c(3000)$, $\Omega_c(3050)$)=$(\frac{1}{2}^-, \frac{3}{2}^-)_{j=1}$ and ($\Omega_c(3066)$, $\Omega_c(3090)$)=$(\frac{3}{2}^-, \frac{5}{2}^-)_{j=2}$. For Ω_b baryons, quark model predicts four $1P$-wave states and their situation is similar with the Ω_c baryons. The splitting of spin-doublets $(\frac{1}{2}^-, \frac{3}{2}^-)_{j=1}$ and $(\frac{3}{2}^-, \frac{5}{2}^-)_{j=2}$ are 7 MeV and 13 MeV(see Table VIII). These four experimental Ω_b states are good candidates of these P-wave doublets, which can be assigned as ($\Omega_b(6315)$, $\Omega_b(6330)$)=$(\frac{1}{2}^-, \frac{3}{2}^-)_{j=1}$ and ($\Omega_b(6340)$, $\Omega_b(6350)$)=$(\frac{3}{2}^-, \frac{5}{2}^-)_{j=2}$. Actually, different collaborations had different conclusions about the quantum numbers of these Ω_c and Ω_b states[91–100] and more theoretical and experimental efforts are needed to assign a proper place in spectra for these P-wave Ω_Q systems.

In quark model scheme, there are two $2S$-wave excitations whose masses are predicted to be 6.446 GeV and 6.466 GeV, respectively. The other collaborations also reported the same results as ours[19], which suggests that these Ω_b states have potentials to be observed at this mass spectra in forthcoming experiments. Finally, the $1D$-wave Ω_Q states also have the possibilities to be found in experiments.

The masses are predicted to be around 3.304 GeV $\sim$ 3.315 GeV for $\Omega_c(1D)$ states and 6.555 GeV $\sim$ 6.562 GeV for $\Omega_b(1D)$ ones.

3.3 Root mean square radius and radial density distributions

Besides of the root mean square radius, we also calculated the radial density distributions which are defined as,

$$\omega(r_\rho) = \int |\Psi(\mathbf{r}_\rho, \mathbf{r}_\lambda)|^2 d\mathbf{r}_\lambda d\Omega_\rho$$
$$\omega(r_\lambda) = \int |\Psi(\mathbf{r}_\rho, \mathbf{r}_\lambda)|^2 d\mathbf{r}_\rho d\Omega_\lambda \tag{42}$$

where Ω_ρ and Ω_λ are the solid angles spanned by vectors $\mathbf{r}_\rho$ and $\mathbf{r}_\lambda$, respectively. As an example, we have shown the results about radial density distributions of Λ_Q baryons in Figs. 10-13.

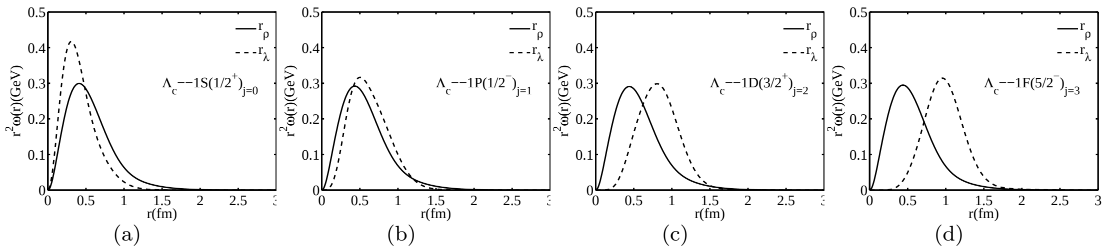

FIG. 10: Radial density distributions for some $1S-1F$ states in the Λ_c families

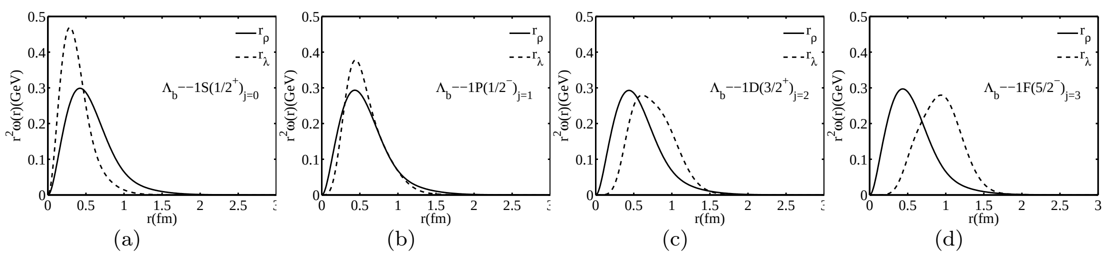

FIG. 11: Radial density distributions for some $1S-1F$ states in the Λ_b families

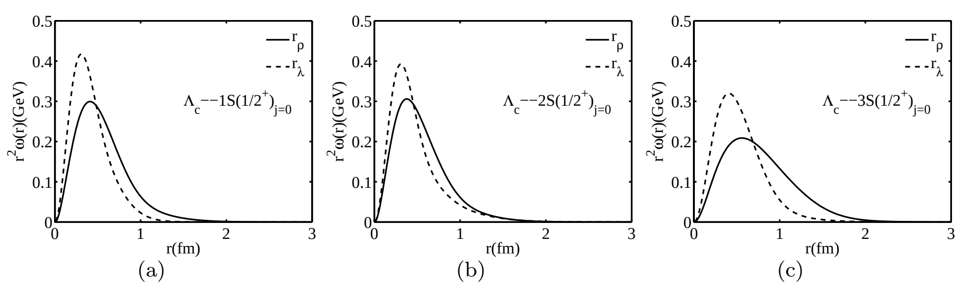

FIG. 12: Radial density distributions for $1S \sim 3S$ states in the Λ_c families.

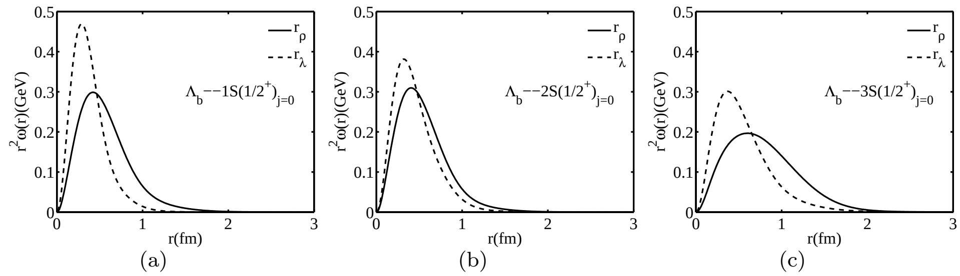

FIG. 13: Radial density distributions for $1S \sim 3S$ states in the Λ_b families.

From Tables III-VIII, we can see the root mean square radius $\langle r_\rho \rangle_{\frac{1}{2}}$ and $\langle r_\lambda \rangle_{\frac{1}{2}}$ of the $1S$ states are 0.39∼0.44 fm and 0.51∼0.63 fm, respectively. For the states with same radial quantum number n, the $\langle r_\lambda \rangle_{\frac{1}{2}}$ becomes larger when the orbital angular momentum L increases. However, $\langle r_\rho \rangle_{\frac{1}{2}}$ remains almost unchanged. This feature is consistent with the results shown in Figs. 10-11, where the peak of $\omega(r_\lambda)$ shifts outward with L increment and $\omega(r_\rho)$ changes little. For the states with same angular momentum L, both $\langle r_\rho \rangle_{\frac{1}{2}}$ and $\langle r_\lambda \rangle_{\frac{1}{2}}$ increase with radial quantum numbers n. And the peaks of their density distributions also shift outward obviously as shown in Figs. 12-13.

It is known that the larger the root mean square radius become, the looser the baryons will be. We can see from Tables III-VIII, the mean square radius of the experimentally established baryons are almost less than 0.8 fm. If we roughly take this value as a criterion, all of the predicted states with radius less than 0.8 fm have potentials to be discovered in forthcoming experiments.

4 Regge trajectories of single heavy baryons Λ_Q, Σ_Q and Ω_Q

The well-known Regge theory was first developed by T.Regge in 1959[101, 102], which preceded the QCD. In 1961, Chew and Frautschi extended this theory and found mesons and baryons lie on linear trajectories of the (J,M^2) plane[103, 104], where J is the angular momentum and M is the mass of hadron. The Regge theory is very successful in studying the strong interactions at high energies and it is an indispensable tool in phenomenological studies. Now, it has been widely used to study the hadronic spectra and was commonly called Regge trajectory. Actually, there have been lots of studies based on QCD theory to understand the Regge trajectory[105–108]. Among them, the most simple and straightforward one was proposed by Nambu in 1978[109, 110], where the relation of J and M^2 was described as,

$$J = \frac{M^2}{2\pi\sigma} + c \tag{43}$$

where, σ is the string tension and c is a constant.

In the present work, we obtained the masses of both orbitally and radially excited charmed and bottom baryons up to rather high excitation numbers, which makes it easy for us to construct the baryon Regge trajectories in (J,M^2) plane. First, both charmed and bottom baryons are classified into two groups which have natural and unnatural parities with $P = (-1)^{J-1/2}$ and $P = (-1)^{J+1/2}$[19], respectively. Then, with the predicted mass spectra by quark model, we plot the Regge trajectories in the (J,M^2) plane for Λ_Q, Σ_Q and Ω_Q systems in Figs. 14-19. Here, we use the following definition about the (J,M^2) Regge trajectories[19],

$$J = \alpha M^2 + \alpha_0 \tag{44}$$

where α and α_0 are slope and intercept. In these figures, the masses calculated in our model are denoted by diamonds and the experimental data are shown by inverted triangle with particle names. The straight lines are obtained by linear fitting of the predicted values. The fitted slopes and intercepts of the Regge trajectories are listed in **Appendix A.2**(Table IX).

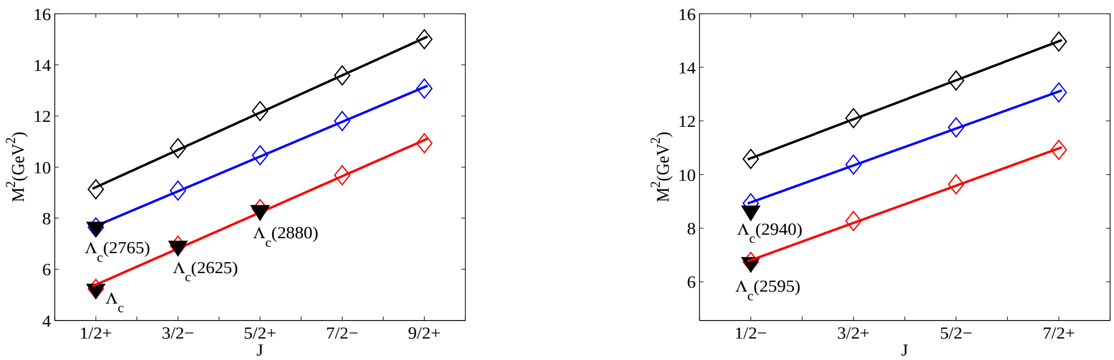

(a) (b)

FIG. 14: Parent and daughter (J,M^2) Regge trajectories for the Λ_c baryons with natural (a) and unnatural (b) parities. Diamonds are predicted masses. Available experimental data are given by inverted triangle with particle names.

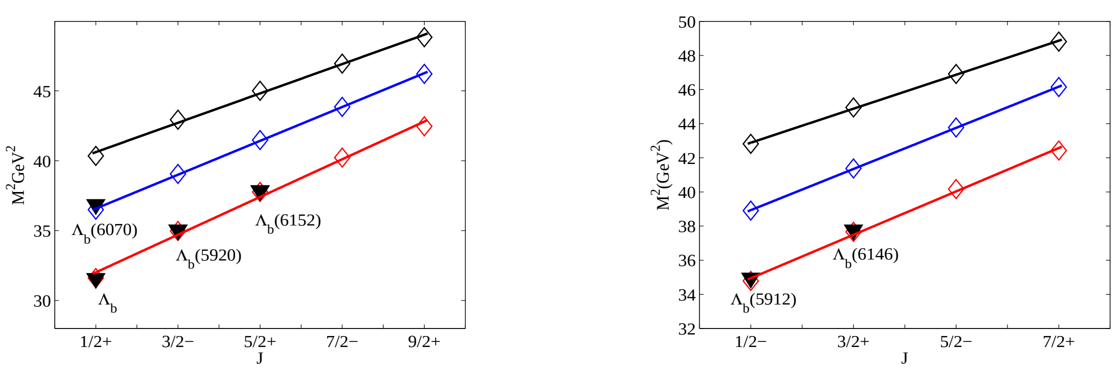

(a) (b)

FIG. 15: Same as in FIG.10 for the Λ_b baryons

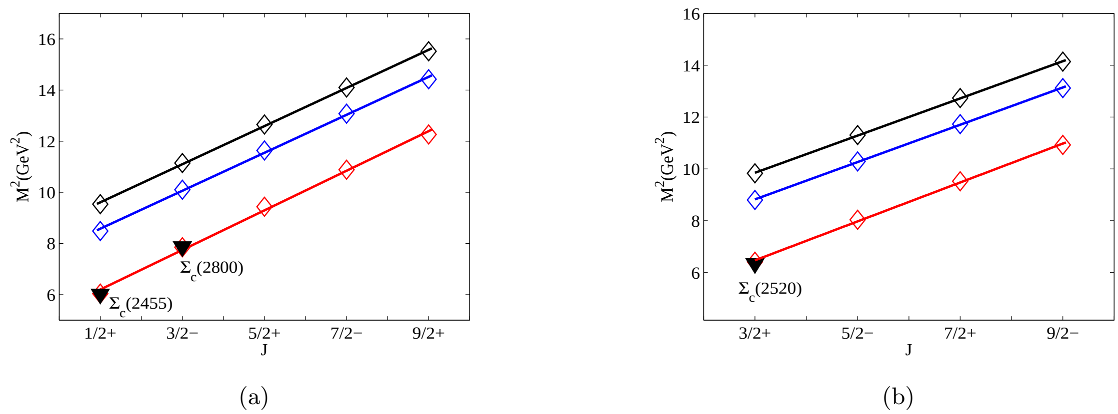

FIG. 16: Same as in FIG.10 for the Σ_c baryons

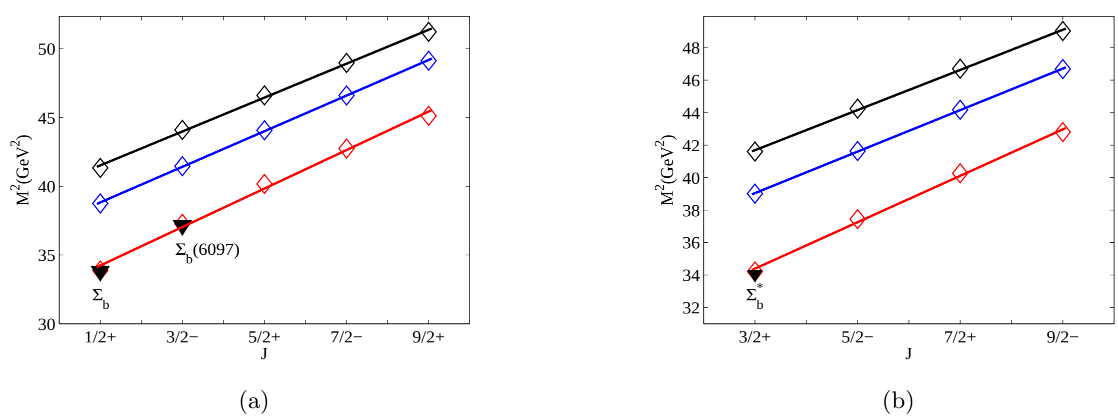

FIG. 17: Same as in FIG.10 for the Σ_b baryons

We can see from these figures that all of the predicted masses in our model fit nicely to the linear trajectories in the (J,M^2) plane. These results can help us to assign an accurate position in the mass spectra for observed baryons. There are two trajectories for which three experimental candidates are available. They are the parent trajectories for $\Lambda_c(\frac{1}{2}^+)$ in Fig. 14(a) and $\Lambda_b(\frac{1}{2}^+)$ in Fig. 15(a). There are several trajectories with two experimental candidates such as the parent trajectory for $\Lambda_c(\frac{1}{2}^-)$ in Fig. 14(b), the parent trajectories for $\Sigma_c(2455)(\frac{1}{2}^+)$ and $\Sigma_b(\frac{1}{2}^+)$ in Figs. 16(a) and 17(a), the parent trajectories for $\Omega_c(\frac{1}{2}^+)$, $\Omega_c(2770)(\frac{3}{2}^+)$ and $\Omega_b(\frac{1}{2}^+)$ in Figs. 18(a), 18(b) and 19(a). All the experimental data coincide well with the corresponding Regge trajectories obtained in present work. Especially, the experimental data for $\Lambda_c(2765)$ and $\Lambda_b(6070)$ fit well with the Regge trajectories in Fig. 14(a) and Fig. 15(a), which suggests that they can be accommodated in the mass spectra as the $2S(\frac{1}{2}^+)$ state. We can see from Fig. 14(b), if $\Lambda_c(2940)$ is interpreted as a $2P(\frac{1}{2}^-)$ state, the predicted mass is about $40 \sim 50$ MeV heavier than the experimental data. On the other hand, the

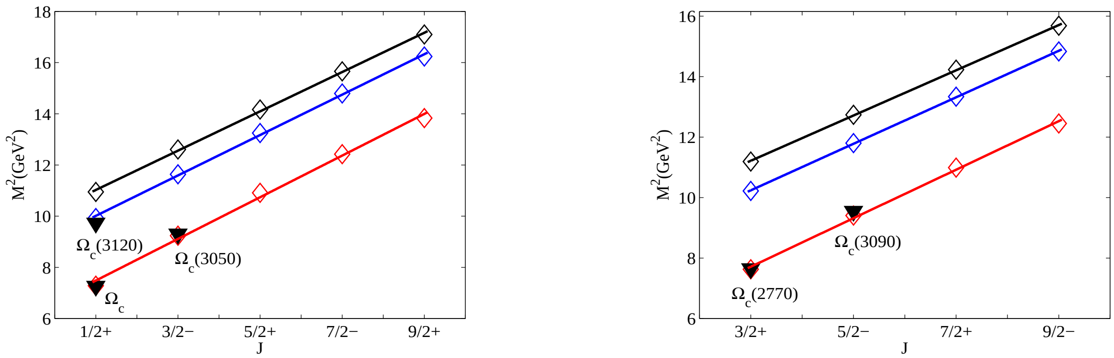

(a) (b)

FIG. 18: Same as in FIG.10 for the Ω_c baryons

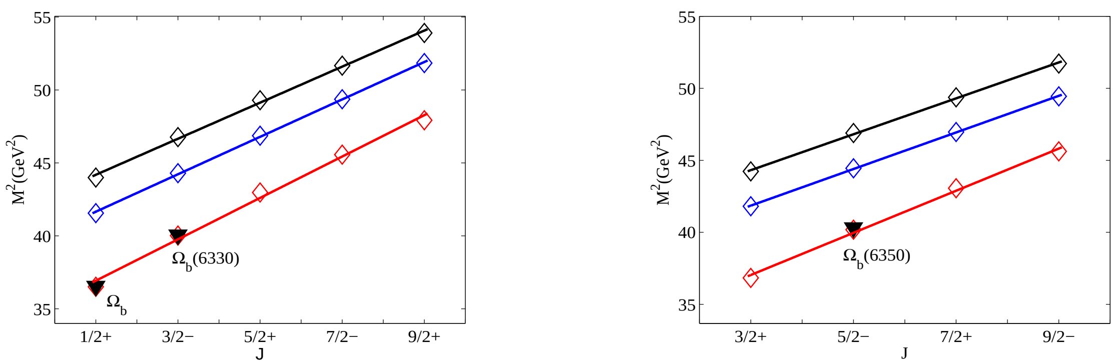

(a) (b)

FIG. 19: Same as in FIG.10 for the Ω_b baryons

Regge trajectories in Fig. 16(a) and Fig. 17(a) show that it is reasonable to assign $\Sigma_c(2800)$ and $\Sigma_b(6097)$ as the $1P(\frac{3}{2}^-)$ state. Finally, the $\Omega_c(3120)$ can be viewed as the first radial excitations$(2S)$ of Ω_c with quantum numbers $\frac{1}{2}^+$ according to the first daughter Regge trajectory in Fig. 18(a). As for the other four observed Ω_c states, the Regge trajectories support assigning $\Omega_c(3050)$ and $\Omega_c(3090)$ as the first orbital excited states$(1P)$ with quantum numbers $\frac{3}{2}^-$ and $\frac{5}{2}^-$, respectively. From Figs. 19(a) and (b), we can see that the situation about $\Omega_b(6330)$ and $\Omega_b(6350)$ is similar with Ω_c. These two states can be interpreted as the $1P$-wave partners of Ω_c with $J^P = \frac{3}{2}^-$ and $\frac{5}{2}^-$.

5 Conclusions

In this work, we have systematically investigate the mass spectra of the single heavy baryons Λ_Q, Σ_Q, and Ω_Q. The first feature of this work in studying the mass spectra is that all parameters such as quark masses and parameters of the interquark potential were determined previously according to the ground states of the baryons. Second, the masses and root mean square radius of the ground states and the states up to rather high orbital and radial excitations are systematically studied(in Tables III-VIII). In addition, with the predicted mass spectra, we construct the Regge trajectories in (J,M^2) plane. It is found that the available experimental data nicely fit to the Regge trajectories, which suggests our assignments for the excited heavy baryons are reasonable. In summary, we have obtained the followings:

(1)We have studied the dependencies on the heavy quark mass m_Q of the λ-mode, ρ-mode and λ-ρ mixing mode to see the features of the single heavy baryons. The results show that mixing of these different excited modes is suppressed and only λ-mode dominates. Basing on this mechanism, we obtained the mass spectra of the Λ_Q, Σ_Q, and Ω_Q baryons with λ excitations. It is found that all currently available experimental data can be well reproduced.

(2)We also investigate the root mean square radius and the radial density distributions of the single heavy baryons. We hope these analysis can help us to predict the upper limit of the mass spectra and to search for baryons which have potentials to be found in experiments.

(3)With the predicted masses, we construct the Regge trajectories in (J,M^2) plane and also obtain the slopes and intercepts of the Regge trajectories. Both the predicted masses and the experimental data fit nicely to the linear trajectories in (J,M^2) plane.

(4)According to the predicted mass spectra, a number of experimental states without spin-parity assignments are successfully distinguished and a number of single heavy barons which have good potentials to be discovered in forthcoming experiments are predicted by quark model.

[1] H. Albrecht *et al.* [ARGUS Collaboration], Phys. Lett. B 317, 227 (1993).
[2] P. L. Frabetti *et al.* [E687 Collaboration], Phys. Rev. Lett. 72, 961(1994).
[3] R. Aaij *et al.* (LHCb Collaboration), Phys. Rev. Lett. 109, 172003 (2012).
[4] T. A. Aaltonen *et al.* (CDF Collaboration), Phys. Rev. D 88, 071101 (2013).
[5] P. A. Zyla *et al.*(Particle Data Group), Prog. Theor. Exp. Phys. 2020, 083C01(2020) and 2021 update.
[6] K. Nakamura *et al.*(Particle Data Group), J.Phys.G 37, 075021(2010).
[7] A. Abdesselam *et al.* [Belle Collaboration], arXiv:1908.06235.
[8] B. Aubert *et al.* [BaBar Collaboration], Phys. Rev. Lett. 98, 012001 (2007).
[9] K. Abe *et al.* [Belle Collaboration], Phys. Rev. Lett. 98, 262001 (2007).
[10] R. Aaij *et al.* [LHCb Collaboration], JHEP 1705, 030 (2017).
[11] R. Aaij *et al.* [LHCb Collaboration], J. High Energy Phys. 06, 136(2020).
[12] R. Aaij *et al.* (LHCb Collaboration), Phys. Rev. Lett. 123, 152001(2019).
[13] R. Mizuk*et al.* [Belle Collaboration], Phys. Rev. Lett. 94, 122002 (2005).
[14] R. Aaij *et al.* (LHCb Collaboration), Phys. Rev. Lett. 122, 012001(2019).
[15] R. Aaij *et al.*(LHCb Collaboration), Phys. Rev. Lett. 124, 082002(2020).

[16] R. Aaij *et al.* [LHCb Collaboration], arXiv:1703.04639[hep-ex].

[17] S. Godfrey and N. Isgur, Phys. Rev. D 32, 189(1985).

[18] S. Capstick and N. Isgur, Phys. Rev. D 34, 2809 (1986); AIPConf. Proc. 132, 267(1985).

[19] D. Ebert, R. N. Faustov, and V. O. Galkin, Phys. Rev. D 84, 014025(2011).

[20] W. Roberts and M. Pervin, Int. J. Mod. Phys. A 23, 2817(2008).

[21] T. Yoshida, E. Hiyama, A. Hosaka, *et al.*, Phys. Rev. D 92, 114029(2015).

[22] K. L. Wang, Q. F. Lü, and X. H. Zhong, Phys. Rev. D 100, 114035(2019).

[23] L. A. Copley, N. Isgur, and G. Karl, Phys. Rev. D 20, 768(1979); 23, 817(E)(1981).

[24] K. Maltman and N. Isgur, Phys. Rev. D 22, 1701(1980).

[25] D. Ebert, R. N. Faustov, and V. O. Galkin, Phys. Rev. D 72, 034026(2005).

[26] D. Ebert, R. N. Faustov, and V. O. Galkin, Phys. Lett. B 659, 612(2008).

[27] H. Garcilazo, J. Vijande, and A. Valcarce, J. Phys. G 34, 961(2007).

[28] M. Karliner and J. L. Rosner, Phys. Rev. D 92, 074026(2015).

[29] K. Thakkar, Z. Shah, A. K. Rai, *et al.*, Nucl. Phys. A 965, 57(2017).

[30] Z. Shah, K. Thakkar, A. K. Rai, *et al.*, Chin. Phys. C 40, 123102(2016).

[31] Z. Shah, K. Thakkar, A. Kumar Rai, *et al.*, Eur. Phys. J. A 52, 313(2016).

[32] F. Hussain, J. G. Korner, and S. Tawfiq, Phys. Rev. D 61, 114003(2000).

[33] M. A. Ivanov, J. G. Korner, and V. E. Lyubovitskij, Phys.Lett. B 448, 143(1999).

[34] M. A. Ivanov, J. G. Korner, V. E. Lyubovitskij, *et al.*, Phys. Rev. D 60, 094002(1999).

[35] C. Albertus, E. Hernandez, J. Nieves, *et al.*, Phys. Rev. D 72, 094022(2005).

[36] S. Migura, D. Merten, B. Metsch, *et al.*, Eur. Phys. J.A 28, 41(2006).

[37] X. H. Zhong and Q. Zhao, Phys. Rev. D 77, 074008(2008).

[38] E. Hernandez and J. Nieves, Phys. Rev. D 84, 057902(2011).

[39] L. H. Liu, L. Y. Xiao, and X. H. Zhong, Phys. Rev. D 86, 034024(2012).

[40] B. Chen, K. W. Wei, X. Liu, and T. Matsuki, Eur. Phys. J. C 77, 154(2017).

[41] B. Chen and X. Liu, Phys. Rev. D 98, 074032(2018).

[42] H. Nagahiro, S. Yasui, A. Hosaka, M. Oka, and H. Noumi, Phys. Rev. D 95, 014023(2017).

[43] Y. X. Yao, K. L. Wang, and X. H. Zhong, Phys. Rev. D 98, 076015(2018).

[44] A. Valcarce, H. Garcilazo, and J. Vijande, Eur. Phys. J. A37, 217(2008).

[45] M. Q. Huang, Y. B. Dai, and C. S. Huang, Phys. Rev. D 52, 3986(1995); 55, 7317(E)(1997).

[46] M. C. Banuls, A. Pich, and I. Scimemi, Phys. Rev. D 61, 094009(2000).

[47] H. Y. Cheng and C. K. Chua, Phys. Rev. D 75, 014006(2007).

[48] N. Jiang, X. L. Chen, and S. L. Zhu, Phys. Rev. D 92, 054017(2015).

[49] H. Y. Cheng and C. K. Chua, Phys. Rev. D 92, 074014(2015).

[50] Y. Kawakami and M. Harada, Phys. Rev. D 99, 094016(2019).

[51] M. Padmanath, R. G. Edwards, N. Mathur, and M. Peardon, arXiv:1311.4806(2013).

[52] H. Bahtiyar, K. U. Can, G. Erkol, and M. Oka, Phys. Lett. B747, 281(2015).

[53] P. Perez-Rubio, S. Collins, and G. S. Bali, Phys. Rev. D 92,034504(2015).

[54] H. Bahtiyar, K. U. Can, G. Erkol, M. Oka, and T. T.Takahashi, Phys. Lett. B 772, 121(2017).

[55] S. L. Zhu and Y. B. Dai, Phys. Rev. D 59, 114015(1999).

[56] S. S. Agaev, K. Azizi, and H. Sundu, Phys. Rev. D 96, 094011(2017).

[57] H. X. Chen, Q. Mao, W. Chen, A. Hosaka, X. Liu, and S. L.Zhu, Phys. Rev. D 95, 094008(2017).

[58] Z. G. Wang, Phys. Rev. D 81, 036002(2010).

[59] Z. G. Wang, Eur. Phys. J. A 44, 105(2010).

[60] T. M. Aliev, K. Azizi, and H. Sundu, Eur. Phys. J. C 75, 14(2015).

[61] T. M. Aliev, T. Barakat, and M. Savci, Phys. Rev. D 93, 056007(2016).

[62] T. M. Aliev, K. Azizi, Y. Sarac, and H. Sundu, Phys. Rev. D 99, 094003(2019).

[63] S. L. Zhu, Phys. Rev. D 61, 114019(2000).

[64] Z. G. Wang, Eur. Phys. J. A 47, 81(2011).

[65] Q. Mao, H. X. Chen, W. Chen, A. Hosaka, X. Liu, and S. L.Zhu, Phys. Rev. D 92, 114007(2015).

[66] H. X. Chen, Q. Mao, A. Hosaka, X. Liu, and S. L. Zhu,Phys. Rev. D 94, 114016(2016).

[67] Z. G. Wang, Nucl. Phys. B 926, 467(2018).

[68] Q. Mao, H. X. Chen, A. Hosaka, X. Liu, and S. L. Zhu,Phys. Rev. D 96, 074021(2017).

[69] T. M. Aliev, K. Azizi, Y. Sarac, and H. Sundu, Phys. Rev. D 98, 094014(2018).

[70] E. L. Cui, H. M. Yang, H. X. Chen, and A. Hosaka, Phys.Rev. D 99, 094021(2019).

[71] K. Azizi, Y. Sarac, and H. Sundu, Phys. Rev. D 101, 074026(2020).

[72] X. Liu, H. X. Chen, Y. R. Liu, A. Hosaka and S. L. Zhu, Phys. Rev. D 77, 014031(2008).

[73] Francisco O. Duraes, Marina Nielsen, Phys. Lett. B 658, 40(2007).

[74] J. R. Zhang, M. Q. Huang, Phys. Rev. D 77, 094002(2008).

[75] J. R. Zhang, M. Q. Huang, Phys. Rev. D 78, 094015(2008).

[76] Z. G. Wang, Chin. Phys. C 45, 013109(2021).

[77] Z. G. Wang, Eur. Phys. J. C 68, 479(2010).

[78] Z. G. Wang, Eur. Phys. J. C 75, 359(2015).

[79] Z. G. Wang, Phys. Lett. B 685, 59(2010).

[80] Z. G. Wang, Eur. Phys. J. C 77, 325(2017).

[81] Z. G. Wang, Int. J. Mod. Phys. A 35, 2050043(2020).

[82] G. L. Yu, Z. G. Wang, arXiv:2109.02217(2021).

[83] B. Chen, K.W. Wei and A. Zhang, Eur. Phys. J. A 51, 82(2015).

[84] Q. F. Lü, D. Y. Chen, and Y. B. Dong, Eur. Phys. J. C 80, 871 (2020).

[85] Q. F. Lü, D. Y. Chen, and Y. B. Dong, *et al*. Phys. Rev. D 104, 054026 (2021)

[86] Q. F. Lü, D. Y. Chen, and Y. B. Dong, Phys. Rev. D 102, 074021 (2020)

[87] E. Hiyama, Y. Kin, and M. Kamimura, Prog. Part. Nucl. Phys. 51, 223(2003)

[88] K. Azizi, Y. Sarac, H. Sundu, Phys. Rev. D 102, 034007(2020).

[89] Y. Huang, C.J. Xiao, L.S. Geng, *et al*., Phys. Rev. D 99, 014008(2019).

[90] R. Aaij et al.(LHCb Collaboration), Phys. Rev. Lett. 122, 012001(2019).

[91] Z. Zhao, D. D. Ye, A. Zhang, Phys. Rev. D 95, 114024 (2017).

[92] B. Chen, X. Liu, Phys. Rev. D 96, 094015 (2017).

[93] M. Padmanath, Nilmani Mathur, Phys. Rev. Lett. 119, 042001 (2017).

[94] K. L. Wang, L. Y. Xiao, X. H. Zhong, *et al*., Phys. Rev. D 95, 116010 (2017).

[95] H. X. Chen, Q. Mao, W. Chen, *et al*., Phys. Rev. D 95, 094008 (2017)

[96] G. Yang, J. L. Ping, Phys. Rev. D 97, 034023 (2018).

[97] H. M. Yang, H. X. Chen, Phys. Rev. D 104, 034037 (2021).

[98] W. Liang, Q. F. Lü, arXiv:2001.02221(2020).

[99] L. Y. Xiao, K. L. Wang, M. S. Liu, *et al.*, arXiv:2001.05110(2020).

[100] Halil Mutuk, Eur. Phys. J. A 56, 146 (2020).

[101] T. Regge, Nuovo Cim. 14, 951(1959).

[102] T. Regge, Nuovo Cim. 18, 947(1960).

[103] G. F. Chew, S. C. Frautschi, Phys. Rev. Lett. 7, 394(1961).

[104] G. F. Chew, S. C. Frautschi, Phys. Rev. Lett. 8, 41 (1962).

[105] G. S. Bali, Phys. Rept. 343, 1, arXiv:hep-ph/0001312(2001).

[106] D. V. Bugg, Four sorts of meson, Phys. Rept. 397, 257, arXiv:hep-ex/0412045(2004).

[107] E. Klempt, A. Zaitsev, Phys. Rept. 454, 1, arXiv:0708.4016(2007).

[108] W. Lucha, F. F. Schoberl, D. Gromes, Phys. Rept. 200, 127(1991).

[109] Y. Nambu, Phys. Rev. D 10, 4262(1974).

[110] Y. Nambu, Phys. Lett. B 80, 372(1979).

[111] K. L. Wang, Q. F. Lü and X. H. Zhong, Rev. D 99, 014011 (2019).

[112] B. Chen, S. Q. Luo, X. Liu, *et al.*, Phys. Rev. D 100, 094032(2019).

[113] Q. F. Lü, L. Y. Xiao, Z. Y. Wang and X. H. Zhong, Eur. Phys. J. C 78,599(2018).

[114] W. Liang, Q. F. Lü and X. H. Zhong, Phys. Rev. D 100, 054013(2019).

[115] Q. F. Lü and X. H. Zhong, arXiv:1910.06126(2019).

[116] S. Godfrey and K. Moats, Phys. Rev. D 93, 034035(2016).

[117] S. Godfrey, K. Moats, and E. S. Swanson, Phys. Rev. D 94, 054025(2016).

[118] W. Liang, Q. F. Lü, arXiv:2004.13568(2020).

[119] H. M. Yang, H. X. Chen, Phys. Rev. D 104, 034037(2021).

[120] K. L. Wang, Y. X. Yao, X. H. Zhong, *et al.*, Phys. Rev. D 96, 116016(2017).

[121] H. X. Chen, Q. Mao, W. Chen, *et al.*, Phys. Rev. D 95, 094008 (2017).

Appendix: A

A.1 The mass spectra and root mean square radius

TABLE III: The root mean square radius (fm) and the mass spectrum (MeV) of the Λ_c family

$l_\rho\ l_\lambda\ L\ s\ j$	$nL(J^P)$	$\langle r_\rho^2\rangle^{\frac{1}{2}}$	$\langle r_\lambda^2\rangle^{\frac{1}{2}}$	M	M_{exp}	[19]	[20]	[18]	[36]	[27]	[67, 76–78]
0 0 0 0 0	$1S(\frac{1}{2}^+)$	0.51	0.44	2288	2286.46[5]	2286	2268	2265	2272	2292	2240±90[76]
	$2S(\frac{1}{2}^+)$	0.63	0.79	2764	2766.6[5]	2769	2791	2775	2769	2669	2780±80[76]
	$3S(\frac{1}{2}^+)$	0.99	0.63	3022		3130					
	$4S(\frac{1}{2}^+)$	0.69	1.13	3135		3437					
0 1 1 0 1	$1P(\frac{1}{2}^-)$	0.53	0.63	2596	2592.25[5]	2598	2625	2630	2594	2559	2610±210[77]
	$2P(\frac{1}{2}^-)$	0.60	0.96	2988	2939.3[6]	2983	2816	2780	2853	2779	
	$3P(\frac{1}{2}^-)$	1.04	0.82	3253		3303					
	$4P(\frac{1}{2}^-)$	0.68	1.26	3308		3588					
0 1 1 0 1	$1P(\frac{3}{2}^-)$	0.55	0.66	2631	2628.1[5]	2627	2636	2640	2586	2559	2620±180[78]
	$2P(\frac{3}{2}^-)$	0.60	0.99	3013		3005	2830	2840	2874	2779	
	$3P(\frac{3}{2}^-)$	1.06	0.83	3277		3322					
	$4P(\frac{3}{2}^-)$	0.67	1.25	3325		3606					
0 2 2 0 2	$1D(\frac{3}{2}^+)$	0.55	0.83	2875	2856.1[5]	2874	2887	2910	2848	2906	2830^{+150}_{-240}[67]
	$2D(\frac{3}{2}^+)$	0.59	1.17	3220		3189	3073	3035	3100	3061	
	$3D(\frac{3}{2}^+)$	0.96	1.12	3479		3480					
	$4D(\frac{3}{2}^+)$	0.82	1.20	3497		3747					
0 2 2 0 2	$1D(\frac{5}{2}^+)$	0.56	0.85	2891	2881.63[5]	2880	2887	2910			2880^{+180}_{-290}[67]
	$2D(\frac{5}{2}^+)$	0.59	1.21	3234		3209					
	$3D(\frac{5}{2}^+)$	1.00	1.09	3492		3500					
	$4D(\frac{5}{2}^+)$	0.77	1.21	3509		3767					
0 3 3 0 3	$1F(\frac{5}{2}^-)$	0.56	1.00	3104		3097	2872	2900			
	$2F(\frac{5}{2}^-)$	0.59	1.43	3429		3375					
	$3F(\frac{5}{2}^-)$	0.70	1.30	3675		3646					
	$4F(\frac{5}{2}^-)$	1.05	1.09	3692		3900					
0 3 3 0 3	$1F(\frac{7}{2}^-)$	0.56	1.02	3111		3078					
	$2F(\frac{7}{2}^-)$	0.60	1.45	3435		3393					
	$3F(\frac{7}{2}^-)$	0.84	1.24	3685		3667					
	$4F(\frac{7}{2}^-)$	0.95	1.14	3699		3922					
0 4 4 0 4	$1G(\frac{7}{2}^+)$	0.55	1.15	3304		3270					
	$2G(\frac{7}{2}^+)$	0.60	1.69	3614		3546					
	$3G(\frac{7}{2}^+)$	0.88	1.24	3868							
	$4G(\frac{7}{2}^+)$	0.90	1.19	3883							
0 4 4 0 4	$1G(\frac{9}{2}^+)$	0.55	1.16	3306		3284					
	$2G(\frac{9}{2}^+)$	0.60	1.70	3615		3564					
	$3G(\frac{9}{2}^+)$	1.05	1.23	3873							
	$4G(\frac{9}{2}^+)$	0.70	1.18	3891							

TABLE IV: The root mean square radius (fm) and the mass spectrum (MeV) of the Λ_b family

$l_\rho\ l_\lambda\ L\ s\ j$	$nL(J^P)$	$\langle r_\rho^2\rangle^{\frac{1}{2}}$	$\langle r_\lambda^2\rangle^{\frac{1}{2}}$	M	M_{exp}	[19]	[20]	[18]	[27]	[89]	[76, 77]
0 0 0 0 0	$1S(\frac{1}{2}^+)$	0.52	0.41	5622	5619.60[5]	5620	5612	5585	5624	5619.6	5610±120[76]
	$2S(\frac{1}{2}^+)$	0.60	0.72	6041	6072.3[5]	6089	6107				6080±90[76]
	$3S(\frac{1}{2}^+)$	0.95	0.68	6352		6455					
	$4S(\frac{1}{2}^+)$	0.75	1.01	6388		6756					
0 1 1 0 1	$1P(\frac{1}{2}^-)$	0.53	0.58	5898	5912.19[5]	5930	5939	5912	5890		5850±180[77]
	$2P(\frac{1}{2}^-)$	0.58	0.85	6238		6326	6180	5780	5853		
	$3P(\frac{1}{2}^-)$	0.66	1.27	6544		6645					
	$4P(\frac{1}{2}^-)$	1.06	0.75	6566		6917					
0 1 1 0 1	$1P(\frac{3}{2}^-)$	0.54	0.59	5913	5920.09[5]	5942	5941	5920	5890		
	$2P(\frac{3}{2}^-)$	0.58	0.86	6249		6333	6191	5840	5874		
	$3P(\frac{3}{2}^-)$	0.64	1.30	6552		6651					
	$4P(\frac{3}{2}^-)$	1.08	0.73	6575		6922					
0 2 2 0 2	$1D(\frac{3}{2}^+)$	0.54	0.75	6137	6146.2[5, 12, 112]	6190	6181	6145	6246		6010^{+200}_{-120}[66]
	$2D(\frac{3}{2}^+)$	0.56	0.97	6432		6526	6401				
	$3D(\frac{3}{2}^+)$	0.62	1.50	6705		6811					
	$4D(\frac{3}{2}^+)$	1.11	0.83	6757		7060					
0 2 2 0 2	$1D(\frac{5}{2}^+)$	0.54	0.76	6145	6152.5[5, 12, 112]	6196	6183	6165			6010^{+200}_{-130}[66]
	$2D(\frac{5}{2}^+)$	0.56	0.98	6440		6531	6422				
	$3D(\frac{5}{2}^+)$	0.62	1.50	6709		6814					
	$4D(\frac{5}{2}^+)$	1.11	0.84	6763		7063					
0 3 3 0 3	$1F(\frac{5}{2}^-)$	0.54	0.91	6338		6408	6206	6205			
	$2F(\frac{5}{2}^-)$	0.54	1.08	6616		6705					
	$3F(\frac{5}{2}^-)$	0.61	1.63	6849		6964					
	$4F(\frac{5}{2}^-)$	1.13	0.98	6932		7196					
0 3 3 0 3	$1F(\frac{7}{2}^-)$	0.54	0.91	6343		6411					
	$2F(\frac{7}{2}^-)$	0.54	1.09	6622		6708					
	$3F(\frac{7}{2}^-)$	0.61	1.63	6852		6966					
	$4F(\frac{7}{2}^-)$	1.13	0.98	6936		7197					
0 4 4 0 4	$1G(\frac{7}{2}^+)$	0.54	1.05	6514		6598	6433				
	$2G(\frac{7}{2}^+)$	0.53	1.20	6793		6867					
	$3G(\frac{7}{2}^+)$	0.59	1.72	6986							
	$4G(\frac{7}{2}^+)$	1.13	1.11	7093							
0 4 4 0 4	$1G(\frac{9}{2}^+)$	0.54	1.06	6517		6599					
	$2G(\frac{9}{2}^+)$	0.53	1.22	6798		6868					
	$3G(\frac{9}{2}^+)$	0.59	1.72	6989							
	$4G(\frac{9}{2}^+)$	1.13	1.11	7095							

TABLE V: The root mean square radius (fm) and the mass spectrum (MeV) of the Σ_c family

l_ρ l_λ L s j	$nL(J^P)$	$\langle r_\rho^2\rangle^{\frac{1}{2}}$	$\langle r_\lambda^2\rangle^{\frac{1}{2}}$	M	M_{exp}	[19]	[20]	[18]	[36]	[27]	[64, 79]
0 0 0 1 1	$1S(\frac{1}{2}^+)$	0.62	0.45	2457	2453.8[5]	2443	2455	2440	2459	2448	2400±260[79]
	$2S(\frac{1}{2}^+)$	0.86	0.72	2913		2901	2958	2890	2947	2793	
	$3S(\frac{1}{2}^+)$	0.94	0.70	3088		3271					
	$4S(\frac{1}{2}^+)$	0.95	1.05	3295		3581					
0 0 0 1 1	$1S(\frac{3}{2}^+)$	0.64	0.49	2532	2518.5[5]	2519	2519	2495	2539	2505	
	$2S(\frac{3}{2}^+)$	0.83	0.79	2967		2936	2995	2985	3010	2825	
	$3S(\frac{3}{2}^+)$	0.99	0.71	3135		3293					
	$4S(\frac{3}{2}^+)$	0.90	1.09	3328		3598					
0 1 1 1 0	$1P(\frac{1}{2}^-)$	0.68	0.69	2823		2799					
	$2P(\frac{1}{2}^-)$	0.80	1.00	3196		3172					
	$3P(\frac{1}{2}^-)$	1.07	0.84	3353		3488					
	$4P(\frac{1}{2}^-)$	0.83	1.22	3511		3770					
0 1 1 1 1	$1P(\frac{1}{2}^-)$	0.67	0.67	2809		2713	2748	2765	2769	2706	2740±200[64]
	$2P(\frac{1}{2}^-)$	0.80	0.98	3185		3125	2768	2770	2817	2791	
	$3P(\frac{1}{2}^-)$	1.06	0.84	3343		3455					
	$4P(\frac{1}{2}^-)$	0.84	1.22	3501		3743					
0 1 1 1 1	$1P(\frac{3}{2}^-)$	0.68	0.69	2829		2798					
	$2P(\frac{3}{2}^-)$	0.80	1.00	3202		3172					
	$3P(\frac{3}{2}^-)$	1.07	0.85	3358		3486					
	$4P(\frac{3}{2}^-)$	0.83	1.22	3516		3768					
0 1 1 1 2	$1P(\frac{3}{2}^-)$	0.67	0.67	2802	2806[5]	2773	2763	2770	2799	2706	2740±200[64]
	$2P(\frac{3}{2}^-)$	0.80	0.97	3179		3151	2776	2805	2815	2791	
	$3P(\frac{3}{2}^-)$	1.06	0.84	3338		3469					
	$4P(\frac{3}{2}^-)$	0.84	1.23	3496		3753					
0 1 1 1 2	$1P(\frac{5}{2}^-)$	0.68	0.70	2835		2789	2790	2815			
	$2P(\frac{5}{2}^-)$	0.80	1.02	3207		3161					
	$3P(\frac{5}{2}^-)$	1.08	0.85	3362		3475					
	$4P(\frac{5}{2}^-)$	0.82	1.22	3521		3757					
0 2 2 1 1	$1D(\frac{1}{2}^+)$	0.69	0.87	3073		3041					
	$2D(\frac{1}{2}^+)$	0.78	1.22	3413		3370					
	$3D(\frac{1}{2}^+)$	1.12	0.98	3558							
	$4D(\frac{1}{2}^+)$	0.78	1.27	3696							
0 2 2 1 1	$1D(\frac{3}{2}^+)$	0.70	0.88	3084		3043					
	$2D(\frac{3}{2}^+)$	0.78	1.25	3422		3366					
	$3D(\frac{3}{2}^+)$	1.13	0.99	3567							
	$4D(\frac{3}{2}^+)$	0.77	1.25	3709							
0 2 2 1 2	$1D(\frac{3}{2}^+)$	0.69	0.87	3073		3040					
	$2D(\frac{3}{2}^+)$	0.78	1.22	3413		3364					
	$3D(\frac{3}{2}^+)$	1.12	0.98	3558							
	$4D(\frac{3}{2}^+)$	0.78	1.27	3696							
0 2 2 1 2	$1D(\frac{5}{2}^+)$	0.70	0.88	3085		3038	3003	3065			
	$2D(\frac{5}{2}^+)$	0.78	1.25	3423		3365					

$l_\rho\ l_\lambda\ L\ s\ j$	$nL(J^P)$	$\langle r_\rho^2\rangle^{\frac{1}{2}}$	$\langle r_\lambda^2\rangle^{\frac{1}{2}}$	M	[19]	$l_\rho\ l_\lambda\ L\ s\ j$	$nL(J^P)$	$\langle r_\rho^2\rangle^{\frac{1}{2}}$	$\langle r_\lambda^2\rangle^{\frac{1}{2}}$	M	[19]
0 2 2 1 3	$1D(\frac{5}{2}^+)$	0.69	0.87	3072	3023	0 3 3 1 4	$1F(\frac{7}{2}^-)$	0.70	1.04	3299	3227
	$2D(\frac{5}{2}^+)$	0.78	1.22	3411	3349		$2F(\frac{7}{2}^-)$	0.77	1.48	3616	
	$3D(\frac{5}{2}^+)$	1.12	0.98	3557			$3F(\frac{7}{2}^-)$	1.16	1.11	3755	
	$4D(\frac{5}{2}^+)$	0.78	1.27	3695			$4F(\frac{7}{2}^-)$	0.73	1.23	3897	
0 2 2 1 3	$1D(\frac{7}{2}^+)$	0.70	0.89	3086	3013	0 3 3 1 4	$1F(\frac{9}{2}^-)$	0.70	1.05	3305	3209
	$2D(\frac{7}{2}^+)$	0.78	1.25	3425	3342		$2F(\frac{9}{2}^-)$	0.78	1.50	3622	
	$3D(\frac{7}{2}^+)$	1.13	0.99	3569			$3F(\frac{9}{2}^-)$	1.06	1.12	3760	
	$4D(\frac{7}{2}^+)$	0.77	1.25	3712			$4F(\frac{9}{2}^-)$	0.74	1.22	3912	
0 3 3 1 2	$1F(\frac{3}{2}^-)$	0.70	1.04	3299	3288	0 4 4 1 3	$1G(\frac{5}{2}^+)$	0.70	1.19	3501	3495
	$2F(\frac{3}{2}^-)$	0.77	1.48	3617			$2G(\frac{5}{2}^+)$	0.77	1.71	3798	
	$3F(\frac{3}{2}^-)$	1.16	1.11	3755			$3G(\frac{7}{2}^+)$	1.18	1.23	3938	
	$4F(\frac{3}{2}^-)$	0.73	1.23	3898			$4G(\frac{5}{2}^+)$	0.73	1.20	4108	
0 3 3 1 2	$1F(\frac{5}{2}^-)$	0.70	1.04	3304	3283	0 4 4 1 3	$1G(\frac{7}{2}^+)$	0.70	1.20	3502	3483
	$2F(\frac{5}{2}^-)$	0.78	1.50	3621			$2G(\frac{7}{2}^+)$	0.77	1.72	3798	
	$3F(\frac{5}{2}^-)$	1.6	1.12	3759			$3G(\frac{7}{2}^+)$	1.18	1.24	3939	
	$4F(\frac{5}{2}^-)$	0.74	1.22	3910			$4G(\frac{7}{2}^+)$	0.74	1.19	4118	
0 3 3 1 3	$1F(\frac{5}{2}^-)$	0.70	1.04	3299	3254	0 4 4 1 4	$1G(\frac{7}{2}^+)$	0.70	1.19	3501	3444
	$2F(\frac{5}{2}^-)$	0.77	1.48	3617			$2G(\frac{7}{2}^+)$	0.77	1.71	3798	
	$3F(\frac{5}{2}^-)$	1.16	1.11	3755			$3G(\frac{7}{2}^+)$	1.18	1.23	3938	
	$4F(\frac{5}{2}^-)$	0.73	1.23	3898			$4G(\frac{7}{2}^+)$	0.73	1.19	4108	
0 3 3 1 3	$1F(\frac{7}{2}^-)$	0.70	1.05	3305	3253	0 4 4 1 4	$1G(\frac{9}{2}^+)$	0.70	1.20	3502	3442
	$2F(\frac{7}{2}^-)$	0.78	1.50	3621			$2G(\frac{9}{2}^+)$	0.77	1.72	3798	
	$3F(\frac{7}{2}^-)$	1.16	1.12	3760			$3G(\frac{9}{2}^+)$	1.18	1.24	3939	
	$4F(\frac{7}{2}^-)$	0.74	1.22	3911			$4G(\frac{7}{2}^+)$	0.75	1.19	4118	

TABLE VI: The root mean square radius (fm) and the mass spectrum (MeV) of the Σ_b family

l_ρ l_λ L s j	$nL(J^P)$	$\langle r_\rho^2\rangle^{\frac{1}{2}}$	$\langle r_\lambda^2\rangle^{\frac{1}{2}}$	M	M_{exp}	[19]	[20]	[18]	[27]	[89]	[64, 79]
0 0 0 1 1	$1S(\frac{1}{2}^+)$	0.63	0.43	5820	5815.6[5]	5808	5833	5795	5789	5815.5	5800±190[79]
	$2S(\frac{1}{2}^+)$	0.78	0.71	6225		6213	6294				
	$3S(\frac{1}{2}^+)$	1.02	0.59	6430		6575					
	$4S(\frac{1}{2}^+)$	0.85	1.07	6566		6869					
0 0 0 1 1	$1S(\frac{3}{2}^+)$	0.64	0.45	5849	5834.7[5]	5834	5858	5805	5844		
	$2S(\frac{3}{2}^+)$	0.77	0.73	6246		6226	6308				
	$3S(\frac{3}{2}^+)$	1.04	0.60	6450		6583					
	$4S(\frac{3}{2}^+)$	0.83	1.09	6579		6876					
0 1 1 1 0	$1P(\frac{1}{2}^-)$	0.67	0.63	6113		6101					
	$2P(\frac{1}{2}^-)$	0.74	0.89	6447		6440					
	$3P(\frac{1}{2}^-)$	1.09	0.74	6648		6756					
	$4P(\frac{1}{2}^-)$	0.81	1.28	6739		7024					
0 1 1 1 1	$1P(\frac{1}{2}^-)$	0.67	0.62	6107		6095	6099	6070	6039		6000±180[64]
	$2P(\frac{1}{2}^-)$	0.74	0.88	6442		6430	6106				
	$3P(\frac{1}{2}^-)$	1.09	0.74	6643		6742					
	$4P(\frac{1}{2}^-)$	0.81	1.28	6736		7008					
0 1 1 1 1	$1P(\frac{3}{2}^-)$	0.67	0.63	6116		6096	6101	6070	6039		
	$2P(\frac{3}{2}^-)$	0.74	0.89	6450		6430					
	$3P(\frac{3}{2}^-)$	1.09	0.74	6650		6742					
	$4P(\frac{3}{2}^-)$	0.81	1.28	6741		7009					
0 1 1 1 2	$1P(\frac{3}{2}^-)$	0.66	0.62	6104	6098.0[5, 90, 111]	6087	6105				6000±180[64]
	$2P(\frac{3}{2}^-)$	0.74	0.88	6439		6423					
	$3P(\frac{3}{2}^-)$	1.09	0.74	6641		6736					
	$4P(\frac{3}{2}^-)$	0.81	1.28	6734		7003					
0 1 1 1 2	$1P(\frac{5}{2}^-)$	0.67	0.63	6119		6084	6172				
	$2P(\frac{5}{2}^-)$	0.74	0.89	6452		6421					
	$3P(\frac{5}{2}^-)$	1.10	0.74	6652		6732					
	$4P(\frac{5}{2}^-)$	0.81	1.28	6743		6999					
0 2 2 1 1	$1D(\frac{1}{2}^+)$	0.67	0.79	6338		6311					
	$2D(\frac{1}{2}^+)$	0.72	1.02	6639		6636					
	$3D(\frac{1}{2}^+)$	1.03	0.87	6828		3626					
	$4D(\frac{1}{2}^+)$	0.78	1.43	6892		6647					
0 2 2 1 1	$1D(\frac{3}{2}^+)$	0.68	0.80	6344		6326					
	$2D(\frac{3}{2}^+)$	0.72	1.03	6645		6647					
	$3D(\frac{3}{2}^+)$	1.13	0.88	6833							
	$4D(\frac{3}{2}^+)$	0.78	1.43	6896							
0 2 2 1 2	$1D(\frac{3}{2}^+)$	0.68	0.79	6338		6285					
	$2D(\frac{3}{2}^+)$	0.72	1.02	6639		6612					
	$3D(\frac{3}{2}^+)$	1.13	0.88	6828							
	$4D(\frac{3}{2}^+)$	0.78	1.43	6892							
0 2 2 1 2	$1D(\frac{5}{2}^+)$	0.68	0.80	6345		6284					
	$2D(\frac{5}{2}^+)$	0.72	1.03	6646		6612					

l_ρ l_λ L s j	$nL(J^P)$	$\langle r_\rho^2\rangle^{\frac{1}{2}}$	$\langle r_\lambda^2\rangle^{\frac{1}{2}}$	M	[19]	[20]	l_ρ l_λ L s j	$nL(J^P)$	$\langle r_\rho^2\rangle^{\frac{1}{2}}$	$\langle r_\lambda^2\rangle^{\frac{1}{2}}$	M	[19]
	$1D(\frac{5}{2}^+)$	0.68	0.79	6338	6270	6325		$1F(\frac{7}{2}^-)$	0.68	0.95	6538	6472
0 2 2 1 3	$2D(\frac{5}{2}^+)$	0.72	1.02	6639		6598	0 3 3 1 4	$2F(\frac{7}{2}^-)$	0.71	1.18	6827	
	$3D(\frac{5}{2}^+)$	1.13	0.87	6827				$3F(\frac{7}{2}^-)$	1.15	1.01	6998	
	$4D(\frac{5}{2}^+)$	0.78	1.43	6892				$4F(\frac{7}{2}^-)$	0.75	1.52	7041	
	$1D(\frac{7}{2}^+)$	0.68	0.80	6346	6260	6333		$1F(\frac{9}{2}^-)$	0.68	0.96	6542	6459
0 2 2 1 3	$2D(\frac{7}{2}^+)$	0.72	1.03	6647	6590	6554	0 3 3 1 4	$2F(\frac{9}{2}^-)$	0.71	1.19	6833	
	$3D(\frac{7}{2}^+)$	1.13	0.88	6834				$3F(\frac{9}{2}^-)$	1.15	1.02	7002	
	$4D(\frac{7}{2}^+)$	0.78	1.43	6897				$4F(\frac{9}{2}^-)$	0.75	1.51	7045	
	$1F(\frac{3}{2}^-)$	0.68	0.95	6538	6550			$1G(\frac{5}{2}^+)$	0.68	1.09	6715	6749
0 3 3 1 2	$2F(\frac{3}{2}^-)$	0.71	1.18	6827			0 4 4 1 3	$2G(\frac{5}{2}^+)$	0.71	1.37	7006	
	$3F(\frac{3}{2}^-)$	1.15	1.01	6998				$3G(\frac{5}{2}^+)$	1.15	1.57	7155	
	$4F(\frac{3}{2}^-)$	0.75	1.52	7041				$4G(\frac{5}{2}^+)$	0.72	1.53	7187	
	$1F(\frac{5}{2}^-)$	0.68	0.95	6542	6564			$1G(\frac{7}{2}^+)$	0.68	1.09	6718	6761
0 3 3 1 2	$2F(\frac{5}{2}^-)$	0.71	1.19	6832			0 4 4 1 3	$2G(\frac{7}{2}^+)$	0.72	1.39	7009	
	$3F(\frac{5}{2}^-)$	1.15	1.02	7001				$3G(\frac{7}{2}^+)$	1.16	1.16	7158	
	$4F(\frac{5}{2}^-)$	0.75	1.51	7044				$4G(\frac{7}{2}^+)$	0.72	1.52	7190	
	$1F(\frac{5}{2}^-)$	0.68	0.95	6538	6501			$1G(\frac{7}{2}^+)$	0.68	1.09	6715	6688
0 3 3 1 3	$2F(\frac{5}{2}^-)$	0.71	1.18	6827			0 4 4 1 4	$2G(\frac{7}{2}^+)$	0.71	1.37	7006	
	$3F(\frac{5}{2}^-)$	1.15	1.01	6998				$3G(\frac{7}{2}^+)$	1.15	1.16	7155	
	$4F(\frac{5}{2}^-)$	0.75	1.52	7041				$4G(\frac{7}{2}^+)$	0.72	1.53	7187	
	$1F(\frac{7}{2}^-)$	0.68	0.95	6542	6500			$1G(\frac{9}{2}^+)$	0.68	1.09	6718	6688
0 3 3 1 3	$2F(\frac{7}{2}^-)$	0.71	1.19	6832			0 4 4 1 4	$2G(\frac{9}{2}^+)$	0.72	1.39	7009	
	$3F(\frac{7}{2}^-)$	1.15	1.02	7001				$3G(\frac{9}{2}^+)$	1.16	1.16	7158	
	$4F(\frac{7}{2}^-)$	0.75	1.51	7045				$4G(\frac{9}{2}^+)$	0.72	1.52	7190	

TABLE VII: The root mean square radius (fm) and the mass spectrum (MeV) of the Ω_c family

l_ρ l_λ L s j	$nL(J^P)$	$\langle r_\rho^2\rangle^{\frac{1}{2}}$	$\langle r_\lambda^2\rangle^{\frac{1}{2}}$	M	M_{exp}	[19]	[20]	[36]	[27]	[64, 80]
0 0 0 1 1	$1S(\frac{1}{2}^+)$	0.55	0.41	2699	2695.2[5]	2698	2718	2688	2710	
	$2S(\frac{1}{2}^+)$	0.78	0.68	3150	3119.1[5]	3088	3152	3169	3044	
	$3S(\frac{1}{2}^+)$	0.88	0.65	3308		3489				
	$4S(\frac{1}{2}^+)$	0.88	1.02	3526		3814				
0 0 0 1 1	$1S(\frac{3}{2}^+)$	0.57	0.46	2762	2765.9[5]	2768	2776	2721	2759	
	$2S(\frac{3}{2}^+)$	0.77	0.73	3197		3123	3190		3080	
	$3S(\frac{3}{2}^+)$	0.92	0.66	3346		3510				
	$4S(\frac{3}{2}^+)$	0.83	1.08	3557		3830				
0 1 1 1 0	$1P(\frac{1}{2}^-)$	0.62	0.65	3057		3055	2977		2959	3050±110[80]
	$2P(\frac{1}{2}^-)$	0.73	0.93	3426		3435	2990		3029	
	$3P(\frac{1}{2}^-)$	1.02	0.79	3562		3754				
	$4P(\frac{1}{2}^-)$	0.76	1.26	3735		4037				
0 1 1 1 1	$1P(\frac{1}{2}^-)$	0.61	0.63	3045	3000.4[5]	2966				2980±160[64]
	$2P(\frac{1}{2}^-)$	0.73	0.92	3416		3384				
	$3P(\frac{1}{2}^-)$	1.01	0.79	3554		3717				
	$4P(\frac{1}{2}^-)$	0.76	1.26	3728		4009				
0 1 1 1 1	$1P(\frac{3}{2}^-)$	0.62	0.65	3062	3050.2[5]	3054	2986		2959	3060±110[80]
	$2P(\frac{3}{2}^-)$	0.73	0.94	3431		3433	2994		3029	
	$3P(\frac{3}{2}^-)$	1.02	0.80	3566		3757				
	$4P(\frac{3}{2}^-)$	0.75	1.26	3739		4036				
0 1 1 1 2	$1P(\frac{3}{2}^-)$	0.61	0.63	3039	3065.5[5]	3029				3060±100[80]
	$2P(\frac{3}{2}^-)$	0.73	0.91	3411		3415				
	$3P(\frac{3}{2}^-)$	1.01	0.78	3550		3737				
	$4P(\frac{3}{2}^-)$	0.77	1.26	3725		4023				
0 1 1 1 2	$1P(\frac{5}{2}^-)$	0.62	0.66	3067	3090.0[5]	3051	3014			3110±100[80]
	$2P(\frac{5}{2}^-)$	0.73	0.94	3435		3427				
	$3P(\frac{5}{2}^-)$	1.02	0.80	3569		3744				
	$4P(\frac{5}{2}^-)$	0.75	1.26	3742		4028				
0 2 2 1 1	$1D(\frac{1}{2}^+)$	0.64	0.82	3304		3287				
	$2D(\frac{1}{2}^+)$	0.71	1.13	3641		3623				
	$3D(\frac{1}{2}^+)$	1.07	0.93	3764						
	$4D(\frac{1}{2}^+)$	0.71	1.35	3909						
0 2 2 1 1	$1D(\frac{3}{2}^+)$	0.64	0.84	3313		3298				
	$2D(\frac{3}{2}^+)$	0.71	1.16	3650		3627				
	$3D(\frac{3}{2}^+)$	1.08	0.94	3771						
	$4D(\frac{3}{2}^+)$	0.71	1.34	3917						
0 2 2 1 2	$1D(\frac{3}{2}^+)$	0.64	0.83	3304		3282				
	$2D(\frac{3}{2}^+)$	0.71	1.13	3641		3613				
	$3D(\frac{3}{2}^+)$	1.07	0.93	3764						
	$4D(\frac{3}{2}^+)$	0.71	1.35	3909						
0 2 2 1 2	$1D(\frac{5}{2}^+)$	0.64	0.84	3314		3297	3196			
	$2D(\frac{5}{2}^+)$	0.71	1.16	3651		3626				

$l_\rho\ l_\lambda\ L\ s\ j$	$nL(J^P)$	$\langle r_\rho^2\rangle^{\frac{1}{2}}$	$\langle r_\lambda^2\rangle^{\frac{1}{2}}$	M	[19]	$l_\rho\ l_\lambda\ L\ s\ j$	$nL(J^P)$	$\langle r_\rho^2\rangle^{\frac{1}{2}}$	$\langle r_\lambda^2\rangle^{\frac{1}{2}}$	M	[19]	[20]
0 2 2 1 3	$1D(\frac{5}{2}^+)$	0.64	0.82	3304	3286	0 3 3 1 4	$1F(\frac{9}{2}^-)$	0.65	1.01	3529		3485
	$2D(\frac{5}{2}^+)$	0.71	1.13	3640	3614		$2F(\frac{9}{2}^-)$	0.71	1.41	3852		
	$3D(\frac{5}{2}^+)$	1.07	0.93	3764			$3F(\frac{9}{2}^-)$	1.11	1.09	3960		
	$4D(\frac{5}{2}^+)$	0.71	1.35	3908			$4F(\frac{9}{2}^-)$	0.67	1.30	4101		
0 2 2 1 3	$1D(\frac{7}{2}^+)$	0.64	0.84	3315	3283	0 4 4 1 3	$1G(\frac{5}{2}^+)$	0.65	1.14	3719	3739	
	$2D(\frac{7}{2}^+)$	0.71	1.16	3652	3611		$2G(\frac{5}{2}^+)$	0.71	1.65	4030		
	$3D(\frac{7}{2}^+)$	1.08	0.94	3773			$3G(\frac{5}{2}^+)$	1.13	1.21	4135		
	$4D(\frac{7}{2}^+)$	0.70	1.33	3919			$4G(\frac{5}{2}^+)$	0.64	1.24	4283		
0 3 3 1 2	$1F(\frac{3}{2}^-)$	0.64	1.00	3525	3533	0 4 4 1 3	$1G(\frac{7}{2}^+)$	0.65	1.15	3720	3721	
	$2F(\frac{3}{2}^-)$	0.71	1.39	3847			$2G(\frac{7}{2}^+)$	0.71	1.67	4030		
	$3F(\frac{3}{2}^-)$	1.11	1.08	3957			$3G(\frac{7}{2}^+)$	1.13	1.21	4135		
	$4F(\frac{3}{2}^-)$	0.67	1.33	4091			$4G(\frac{7}{2}^+)$	0.64	1.22	4291		
0 3 3 1 2	$1F(\frac{5}{2}^-)$	0.65	1.00	3528	3522	0 4 4 1 4	$1G(\frac{7}{2}^+)$	0.65	1.14	3719	3707	
	$2F(\frac{5}{2}^-)$	0.71	1.41	3851			$2G(\frac{7}{2}^+)$	0.71	1.65	4030		
	$3F(\frac{5}{2}^-)$	1.11	1.08	3960			$3G(\frac{7}{2}^+)$	1.13	1.21	4135		
	$4F(\frac{5}{2}^-)$	0.67	1.31	4099			$4G(\frac{7}{2}^+)$	0.64	1.24	4283		
0 3 3 1 3	$1F(\frac{5}{2}^-)$	0.64	1.00	3525	3515	0 4 4 1 4	$1G(\frac{9}{2}^+)$	0.64	1.15	3720		3705
	$2F(\frac{5}{2}^-)$	0.71	1.39	3847			$2G(\frac{9}{2}^+)$	0.71	1.67	4030		
	$3F(\frac{5}{2}^-)$	1.11	1.08	3957			$3G(\frac{9}{2}^+)$	1.13	1.21	4135		
	$4F(\frac{5}{2}^-)$	0.67	1.33	4091			$4G(\frac{9}{2}^+)$	0.64	1.22	4291		
0 3 3 1 3	$1F(\frac{7}{2}^-)$	0.65	1.00	3529	3514	0 4 4 1 5	$1G(\frac{9}{2}^+)$	0.65	1.14	3719		3685
	$2F(\frac{7}{2}^-)$	0.71	1.41	3851			$2G(\frac{9}{2}^+)$	0.71	1.65	4030		
	$3F(\frac{7}{2}^-)$	1.11	1.08	3960			$3G(\frac{9}{2}^+)$	1.13	1.20	4135		
	$4F(\frac{7}{2}^-)$	0.67	1.30	4100			$4G(\frac{9}{2}^+)$	0.64	1.24	4283		
0 3 3 1 4	$1F(\frac{7}{2}^-)$	0.64	0.99	3524	3498	0 4 4 1 5	$1G(\frac{11}{2}^+)$	0.65	1.15	3720		3665
	$2F(\frac{7}{2}^-)$	0.71	1.38	3846			$2G(\frac{11}{2}^+)$	0.71	1.67	4030		
	$3F(\frac{7}{2}^-)$	1.11	1.08	3957			$3G(\frac{11}{2}^+)$	1.13	1.21	4135		
	$4F(\frac{7}{2}^-)$	0.67	1.33	4091			$4G(\frac{11}{2}^+)$	0.64	1.22	4292		

TABLE VIII: The root mean square radius (fm) and the mass spectrum (MeV) of the Ω_b family

l_ρ l_λ L s j	$nL(J^P)$	$\langle r_\rho^2\rangle^{\frac{1}{2}}$	$\langle r_\lambda^2\rangle^{\frac{1}{2}}$	M	M_{exp}	[19]	[20]	[27]	[64, 81]
0 0 0 1 1	$1S(\frac{1}{2}^+)$	0.57	0.39	6043	6046.1[5]	6064	6081	6037	
	$2S(\frac{1}{2}^+)$	0.71	0.67	6446		6450	6472		
	$3S(\frac{1}{2}^+)$	0.95	0.55	6633		6804			
	$4S(\frac{1}{2}^+)$	0.79	1.01	6790		7091			
0 0 0 1 1	$1S(\frac{3}{2}^+)$	0.57	0.41	6069		6088	6102	6090	
	$2S(\frac{3}{2}^+)$	0.70	0.69	6466		6461	6478		
	$3S(\frac{3}{2}^+)$	0.97	0.55	6650		6811			
	$4S(\frac{3}{2}^+)$	0.77	1.05	6804		7096			
0 1 1 1 0	$1P(\frac{1}{2}^-)$	0.61	0.58	6334		6339	6301	6278	6320(110)[81]
	$2P(\frac{1}{2}^-)$	0.68	0.83	6662		6710	6312		
	$3P(\frac{1}{2}^-)$	1.04	0.68	6844		7009			
	$4P(\frac{1}{2}^-)$	0.75	1.28	6969		7265			
0 1 1 1 1	$1P(\frac{1}{2}^-)$	0.60	0.58	6329	6315.64[15]	6330			6270±140[64]
	$2P(\frac{1}{2}^-)$	0.68	0.83	6658		6706			
	$3P(\frac{1}{2}^-)$	1.03	0.68	6841		7003			
	$4P(\frac{1}{2}^-)$	0.75	1.28	6966		7257			
0 1 1 1 1	$1P(\frac{3}{2}^-)$	0.61	0.58	6336	6330.30[15]	6340			6310±110[81]
	$2P(\frac{3}{2}^-)$	0.68	0.84	6664		6750			
	$3P(\frac{3}{2}^-)$	1.04	0.69	6846		7002			
	$4P(\frac{3}{2}^-)$	0.75	1.29	6970		7258			
0 1 1 1 2	$1P(\frac{3}{2}^-)$	0.60	0.57	6326	6339.71[15]	6331	6304	6278	6370±90[81]
	$2P(\frac{3}{2}^-)$	0.68	0.83	6655		6699	6311		
	$3P(\frac{3}{2}^-)$	1.03	0.68	6839		6998			
	$4P(\frac{3}{2}^-)$	0.75	1.27	6964		7250			
0 1 1 1 2	$1P(\frac{5}{2}^-)$	0.61	0.59	6339	6349.88[15]	6334	6311		6350±100[81]
	$2P(\frac{5}{2}^-)$	0.68	0.84	6666		6700			
	$3P(\frac{5}{2}^-)$	1.04	0.69	6848		6996			
	$4P(\frac{5}{2}^-)$	0.75	1.29	6972		7251			
0 2 2 1 1	$1D(\frac{1}{2}^+)$	0.62	0.74	6556		6540			
	$2D(\frac{1}{2}^+)$	0.66	0.95	6846		6857			
	$3D(\frac{1}{2}^+)$	1.08	0.82	7021					
	$4D(\frac{1}{2}^+)$	0.73	1.48	7121					
0 2 2 1 1	$1D(\frac{3}{2}^+)$	0.62	0.75	6561		6549			
	$2D(\frac{3}{2}^+)$	0.66	0.95	6852		6863			
	$3D(\frac{3}{2}^+)$	1.08	0.82	7026					
	$4D(\frac{3}{2}^+)$	0.73	1.49	7124					
0 2 2 1 2	$1D(\frac{3}{2}^+)$	0.62	0.74	6556		6530			
	$2D(\frac{3}{2}^+)$	0.66	0.95	6846		6846			
	$3D(\frac{3}{2}^+)$	1.08	0.82	7022					
	$4D(\frac{3}{2}^+)$	0.73	1.48	7121					
0 2 2 1 2	$1D(\frac{5}{2}^+)$	0.62	0.75	6561		6529			
	$2D(\frac{5}{2}^+)$	0.66	0.95	6852		6846			

$l_\rho\ l_\lambda\ L\ s\ j$	$nL(J^P)$	$\langle r_\rho^2\rangle^{\frac{1}{2}}$	$\langle r_\lambda^2\rangle^{\frac{1}{2}}$	M	[19]		$l_\rho\ l_\lambda\ L\ s\ j$	$nL(J^P)$	$\langle r_\rho^2\rangle^{\frac{1}{2}}$	$\langle r_\lambda^2\rangle^{\frac{1}{2}}$	M	[19]
	$4D(\frac{5}{2}^+)$	0.73	1.9	7124								
0 2 2 1 3	$1D(\frac{5}{2}^+)$	0.62	0.74	6555	6520	6492[20]	0 3 3 1 4	$1F(\frac{9}{2}^-)$	0.63	0.91	6754	6713
	$2D(\frac{5}{2}^+)$	0.66	0.95	6846	6837	6494[20]		$2F(\frac{9}{2}^-)$	0.64	1.06	7031	
	$3D(\frac{5}{2}^+)$	1.08	0.81	7021				$3F(\frac{9}{2}^-)$	1.11	0.96	7191	
	$4D(\frac{5}{2}^+)$	0.73	1.48	7121				$4F(\frac{9}{2}^-)$	0.71	1.63	7266	
0 2 2 1 3	$1D(\frac{7}{2}^+)$	0.62	0.75	6562	6517	6497[20]	0 4 4 1 3	$1G(\frac{5}{2}^+)$	0.63	1.05	6923	6952
	$2D(\frac{7}{2}^+)$	0.66	0.95	6853	6834	6667[20]		$2G(\frac{5}{2}^+)$	0.63	1.17	7201	
	$3D(\frac{7}{2}^+)$	1.08	0.82	7027				$3G(\frac{5}{2}^+)$	1.12	1.08	7342	
	$4D(\frac{7}{2}^+)$	0.73	1.49	7125				$4G(\frac{5}{2}^+)$	0.69	1.74	7398	
0 3 3 1 2	$1F(\frac{3}{2}^-)$	0.63	0.90	6751	6763	6370[81]	0 4 4 1 3	$1G(\frac{7}{2}^+)$	0.63	1.05	6925	6959
	$2F(\frac{3}{2}^-)$	0.64	1.05	7026				$2G(\frac{7}{2}^+)$	0.64	1.17	7204	
	$3F(\frac{3}{2}^-)$	1.10	0.95	7188				$3G(\frac{7}{2}^+)$	1.12	1.08	7344	
	$4F(\frac{3}{2}^-)$	0.71	1.64	7264				$4G(\frac{7}{2}^+)$	0.69	1.73	7400	
0 3 3 1 2	$1F(\frac{5}{2}^-)$	0.63	0.91	6754	6771		0 4 4 1 4	$1G(\frac{7}{2}^+)$	0.63	1.05	6923	6916
	$2F(\frac{5}{2}^-)$	0.64	1.06	7031				$2G(\frac{7}{2}^+)$	0.63	1.17	7201	
	$3F(\frac{5}{2}^-)$	1.11	0.96	7191				$3G(\frac{7}{2}^+)$	1.11	1.08	7342	
	$4F(\frac{5}{2}^-)$	0.71	1.63	7265				$4G(\frac{7}{2}^+)$	0.69	1.74	7398	
0 3 3 1 3	$1F(\frac{5}{2}^-)$	0.63	0.90	6751	6737		0 4 4 1 4	$1G(\frac{9}{2}^+)$	0.63	1.05	6925	6915
	$2F(\frac{5}{2}^-)$	0.64	1.05	7026				$2G(\frac{9}{2}^+)$	0.64	1.17	7205	
	$3F(\frac{5}{2}^-)$	1.10	0.95	7188				$3G(\frac{9}{2}^+)$	1.12	1.08	7344	
	$4F(\frac{5}{2}^-)$	0.71	1.64	7264				$4G(\frac{9}{2}^+)$	0.69	1.73	7400	
0 3 3 1 3	$1F(\frac{7}{2}^-)$	0.63	0.91	6754	6736		0 4 4 1 5	$1G(\frac{9}{2}^+)$	0.63	1.04	6922	6892
	$2F(\frac{7}{2}^-)$	0.64	1.06	7031				$2G(\frac{9}{2}^+)$	0.63	1.16	7201	
	$3F(\frac{7}{2}^-)$	1.11	0.96	7191				$3G(\frac{9}{2}^+)$	1.12	1.08	7342	
	$4F(\frac{7}{2}^-)$	0.71	1.63	7266				$4G(\frac{9}{2}^+)$	0.69	1.74	7398	
0 3 3 1 4	$1F(\frac{7}{2}^-)$	0.63	0.90	6750	6719		0 4 4 1 5	$1G(\frac{11}{2}^+)$	0.63	1.05	6925	6884
	$2F(\frac{7}{2}^-)$	0.64	1.05	7026				$2G(\frac{11}{2}^+)$	0.64	1.18	7205	
	$3F(\frac{7}{2}^-)$	1.10	0.95	7188				$3G(\frac{11}{2}^+)$	1.12	1.08	7344	
	$4F(\frac{7}{2}^-)$	0.71	1.64	7264				$4G(\frac{11}{2}^+)$	0.69	1.73	7400	

A.2 Fitted parameters of the Regge trajectories

TABLE IX: Fitted parameters α and α_0 for the slope and intercept of the (J,M^2) parent and daughter Regge trajectories for Λ_Q, Σ_Q and Ω_Q.

Trajectory	$\alpha(\mathrm{Gev}^{-2})$	α_0	$\alpha(\mathrm{Gev}^{-2})$	α_0
	$\Lambda_c(\frac{1}{2}^+)$		$\Lambda_c(\frac{1}{2}^-)$	
parent	0.707±0.009	-3.312±0.005	0.719±0.011	-4.393±0.033
1 daughter	0.736±0.001	-5.166±0.002	0.725±0.003	-5.998±0.018
2 daughter	0.686±0.002	-5.818±0.006	0.687±0.002	-6.790±0.013
	$\Sigma_c(\frac{1}{2}^+)$		$\Sigma_c^*(\frac{3}{2}^+)$	
parent	0.646±0.007	-3.500±0.007	0.666±0.007	-2.811±0.005
1 daughter	0.673±0.003	-5.275±0.011	0.695±0.001	-4.632±0.001
2 daughter	0.670±0.002	-5.940±0.009	0.697±0.001	-5.363±0.003
	$\Omega_c(\frac{1}{2}^+)$		$\Omega_c^*(\frac{3}{2}^+)$	
parent	0.614±0.009	-4.096±0.018	0.623±0.012	-3.306±0.003
1 daughter	0.633±0.002	-5.840±0.012	0.650±0.001	-5.158±0.003
2 daughter	0.651±0.003	-6.673±0.002	0.668±0.001	-5.999±0.005
	$\Lambda_b(\frac{1}{2}^+)$		$\Lambda_b(\frac{1}{2}^-)$	
parent	0.371±0.009	-11.364±0.196	0.393±0.011	-13.240±0.304
1 daughter	0.413±0.012	-14.594±0.012	0.415±0.010	-15.643±0.010
2 daughter	0.476±0.007	-18.843±0.232	0.502±0.003	-21.019±0.131
	$\Sigma_b(\frac{1}{2}^+)$		$\Sigma_b^*(\frac{3}{2}^+)$	
parent	0.357±0.006	-11.729±0.157	0.350±0.010	-10.535±0.202
1 daughter	0.386±0.009	-14.490±0.008	0.391±0.010	-13.775±0.010
2 daughter	0.406±0.002	-16.338±0.077	0.405±0.003	-15.370±0.095
	$\Omega_b(\frac{1}{2}^+)$		$\Omega_b^*(\frac{3}{2}^+)$	
parent	0.352±0.008	-12.517±0.214	0.342±0.012	-11.162±0.278
1 daughter	0.390±0.001	-15.739±0.017	0.393±0.051	-14.965±1.966
2 daughter	0.405±0.002	-17.382±0.087	0.401±0.003	-16.267±0.108

Appendix: B

The coefficient $C_{lm,k}$ and the shift-direction vector $\mathbf{D}_{lm,k}$ in Eqs(38)-(39) are dimensionless numbers independent of ν_n and ϵ, and they can be described as,

$$C_{lm,k} \equiv \sum_{j=0}^{\left[\frac{l-m}{2}\right]} A_{lm,j} \sum_{s=0}^{p} \sum_{t=0}^{q} \sum_{u=0}^{j} (-1)^{l-u-t-s} \binom{p}{s} \binom{q}{t} \binom{j}{u} \tag{45}$$

where $p = l - m - 2j$, $q = j + m$ and

$$\mathbf{D}_{lm,k} \equiv \frac{1}{l}[(2s-p)\mathbf{a}_z + (2t-q)\mathbf{a}_{xy} + (2u-j)\mathbf{a}_{xy}^*] \tag{46}$$

with

$$A_{lm,j} = \Big[\frac{(2l+1)(l-m)!}{4\pi(l+m)!}\Big]^{\frac{1}{2}} \frac{(l+m)!(-1)^j}{(-2)^m 4^j j!(m+j)!(l-m-2j)!} \tag{47}$$

In Eq.(46) $\mathbf{a}_z$, $\mathbf{a}_{xy}$ and $\mathbf{a}_{xy}^*$ are called the shift vectors which are defined as $\mathbf{a}_z \equiv (0,0,1)$, $\mathbf{a}_{xy} \equiv (1,i,0)$, $\mathbf{a}_{xy}^* \equiv (1,-i,0)$. For relation(46) and Eq.(47), when $m < 0$, we should change $A_{lm,j} \to (-1)^m A_{l-m,j}$ and $\mathbf{D} \to \mathbf{D}^*$.

B.1 Three-body matrix elements of the potential energy

In the following, we show how to obtain matrix elements of the various pieces of the Hamiltonian in the Jacobi coordinate channel 3. For most of the terms in the Hamiltonian, they are the form of $\widetilde{H}_{ij}(\boldsymbol{r}_{ij})$, and so we have to integrate functions of $\boldsymbol{r}_{12}$, $\boldsymbol{r}_{13}$ and $\boldsymbol{r}_{23}$, where $\boldsymbol{r}_{12} = \boldsymbol{r}_{\rho_3}$, $\boldsymbol{r}_{13} = \boldsymbol{r}_{\rho_2}$ and $\boldsymbol{r}_{23} = \boldsymbol{r}_{\rho_1}$ in three Jacobi coordinate channels, respectively. The matrix element of $\widetilde{G}(\boldsymbol{r}_{12})$ which is independent of spin and orbital,

$$\begin{aligned}
&\langle[\phi_{n_{\rho_a} l_{\rho_a} m_{l_{\rho_a}}}(\boldsymbol{r}_{\rho_3})\phi_{n_{\lambda_a} l_{\lambda_a} m_{l_{\lambda_a}}}(\boldsymbol{r}_{\lambda_3})]_L|\widetilde{G}(\boldsymbol{r}_{12})|[\phi_{n_{\rho_b} l_{\rho_b} m_{l_{\rho_b}}}(\boldsymbol{r}_{\rho_3})\phi_{n_{\lambda_b} l_{\lambda_b} m_{l_{\lambda_b}}}(\boldsymbol{r}_{\lambda_3})]_L\rangle \\
&= \langle[\phi_{n_{\rho_a} l_{\rho_a} m_{l_{\rho_a}}}(\boldsymbol{r}_{\rho_3})\phi_{n_{\lambda_a} l_{\lambda_a} m_{l_{\lambda_a}}}(\boldsymbol{r}_{\lambda_3})]_L|\widetilde{G}(\boldsymbol{r}_{\rho_3})|[\phi_{n_{\rho_b} l_{\rho_b} m_{l_{\rho_b}}}(\boldsymbol{r}_{\rho_3})\phi_{n_{\lambda_b} l_{\lambda_b} m_{l_{\lambda_b}}}(\boldsymbol{r}_{\lambda_3})]_L\rangle
\end{aligned} \tag{48}$$

can be calculated directly. The matrix elements of $\widetilde{G}(\boldsymbol{r}_{13})$ and $\widetilde{G}(\boldsymbol{r}_{23})$ can be expressed as,

$$\langle[\phi_{n_{\rho_a} l_{\rho_a} m_{l_{\rho_a}}}(\boldsymbol{r}_{\rho_3})\phi_{n_{\lambda_a} l_{\lambda_a} m_{l_{\lambda_a}}}(\boldsymbol{r}_{\lambda_3})]_L|\widetilde{G}(\boldsymbol{r}_{\rho_k})|[\phi_{n_{\rho_b} l_{\rho_b} m_{l_{\rho_b}}}(\boldsymbol{r}_{\rho_3})\phi_{n_{\lambda_b} l_{\lambda_b} m_{l_{\lambda_b}}}(\boldsymbol{r}_{\lambda_3})]_L\rangle_{k=1,2} \tag{49}$$

We have to perform the integration over $\boldsymbol{r}_{\rho_1}$ or $\boldsymbol{r}_{\rho_2}$ in channel 3, which requires the Jacobi coordinate transformations $(\boldsymbol{r}_{\rho_3},\boldsymbol{r}_{\lambda_3}) \to (\boldsymbol{r}_{\rho_k},\boldsymbol{r}_{\lambda_k})_{k=1,2}$. Then, the infinitesimally-shifted Gaussian basis functions in channels 3 are expressed in Jacobi coordinates $(\boldsymbol{r}_{\rho_k},\boldsymbol{r}_{\lambda_k})_{k=1,2}$. The structure of the final expression of the matrix elements about Eqs.(48) and (49) are illustrated explicitly as,

$$
\begin{aligned}
&\langle[\phi_{n_{\rho_a}l_{\rho_a}m_{l_{\rho_a}}}(\boldsymbol{r}_{\rho_3})\phi_{n_{\lambda_a}l_{\lambda_a}m_{l_{\lambda_a}}}(\boldsymbol{r}_{\lambda_3})]_{Lm_L}|\widetilde{G}(\boldsymbol{r}_{\rho_k})|[\phi_{n_{\rho_b}l_{\rho_b}m_{l_{\rho_b}}}(\boldsymbol{r}_{\rho_3})\phi_{n_{\lambda_b}l_{\lambda_b}m_{l_{\lambda_b}}}(\boldsymbol{r}_{\lambda_3})]_{Lm_L}\rangle_{k=1,2}\\
&= N_{n_{\rho_a}l_{\rho_a}}N_{n_{\lambda_a}l_{\lambda_a}}N_{n_{\rho_b}l_{\rho_b}}N_{n_{\lambda_b}l_{\lambda_b}}\frac{1}{(\nu_{n_{\rho_a}})^{l_{\rho_a}}(\nu_{n_{\lambda_a}})^{l_{\lambda_a}}(\nu_{n_{\rho_b}})^{l_{\rho_b}}(\nu_{n_{\lambda_b}})^{l_{\lambda_b}}}4\pi\big(\frac{\pi}{B_{r_k}}\big)^{\frac{3}{2}}\\
&\times\sum_{m_{l_{\rho_a}}m_{l_{\lambda_a}}}(l_{\rho_a}m_{l_{\rho_a}}l_{\lambda_a}m_{l_{\lambda_a}}|Lm_L)\sum_{m_{l_{\rho_b}}m_{l_{\lambda_b}}}(l_{\rho_b}m_{l_{\rho_b}}l_{\lambda_b}m_{l_{\lambda_b}}|Lm_L)\\
&\times\sum_{m=0}^{Lsum}\frac{m!}{(2m+1)!}\int_0^\infty V(r_{\rho_k})Exp(-\alpha_{r_k}r_{\rho_k}^2)r_{\rho_k}^{2m+2}dr_{\rho_k}\\
&\times\sum_{k_aK_ak_bK_b}C_{l_{\rho_a}m_{l_{\rho_a}}k_a}C_{l_{\lambda_a}m_{l_{\lambda_a}}K_a}C_{l_{\rho_b}m_{l_{\rho_b}}k_b}C_{l_{\lambda_b}m_{l_{\lambda_b}}K_b}\\
&\times\sum_{n_{12}=0}^{Lsum-m}\sum_{n_{13}=0}^{Lsum-m}\sum_{n_{14}=0}^{Lsum-m}\sum_{n_{23}=0}^{Lsum-m}\sum_{n_{24}=0}^{Lsum-m}\sum_{n_{34}=0}^{Lsum-m}\sum_{m_{12}=0}^{m}\sum_{m_{13}=0}^{m}\sum_{m_{14}=0}^{m}\sum_{m_{23}=0}^{m}\sum_{m_{24}=0}^{m}\sum_{m_{34}=0}^{m}\\
&\times\frac{\tilde g_{12}^{m_{12}}\tilde g_{13}^{m_{13}}\tilde g_{14}^{m_{14}}\tilde g_{23}^{m_{23}}\tilde g_{24}^{m_{24}}\tilde g_{34}^{m_3}\hat g_{12}^{n_{12}}\hat g_{13}^{n_{13}}\hat g_{14}^{n_{14}}\hat g_{23}^{n_{23}}\hat g_{24}^{n_{24}}\hat g_{34}^{n_{34}}}{n_{12}!n_{13}!n_{14}!n_{23}!n_{24}!n_{34}!m_{12}!m_{13}!m_{14}!m_{23}!m_{24}!m_{34}!}\\
&\times(\mathbf{D}_1\cdot\mathbf{D}_2)^{n_{12}+m_{12}}(\mathbf{D}_1\cdot\mathbf{D}_3)^{n_{13}+m_{13}}(\mathbf{D}_1\cdot\mathbf{D}_4)^{n_{14}+m_{14}}\\
&\times(\mathbf{D}_2\cdot\mathbf{D}_3)^{n_{23}+m_{23}}(\mathbf{D}_2\cdot\mathbf{D}_4)^{n_{24}+m_{24}}(\mathbf{D}_3\cdot\mathbf{D}_4)^{n_{34}+m_{34}}\\
&\times\delta(n_{12}+n_{13}+n_{14}+n_{23}+n_{24}+n_{34}-(Lsum-m))\delta(m_{12}+m_{13}+m_{14}+m_{23}+m_{24}+m_{34}-m)\\
&\times\delta(n_{12}+n_{13}+n_{14}+m_{12}+m_{13}+m_{14}-l_{\rho_a})\delta(n_{12}+n_{23}+n_{24}+m_{12}+m_{23}+m_{24}-l_{\lambda_a})\\
&\times\delta(n_{13}+n_{23}+n_{34}+m_{13}+m_{23}+m_{34}-l_{\rho_b})\delta(n_{14}+n_{24}+n_{34}+m_{14}+m_{24}+m_{34}-l_{\lambda_b})
\end{aligned}
\tag{50}
$$

$$
\begin{aligned}
A_{r_k}&=\nu_{n_{\rho_a}}\alpha_{3k}^{r2}+\nu_{n_{\lambda_a}}\gamma_{3k}^{r2}+\nu_{n_{\rho_b}}\alpha_{3k}^{r2}+\nu_{n_{\lambda_b}}\gamma_{3k}^{r2}\\
B_{r_k}&=\nu_{n_{\rho_a}}\beta_{3k}^{r2}+\nu_{n_{\lambda_a}}\delta_{3k}^{r2}+\nu_{n_{\rho_b}}\beta_{3k}^{r2}+\nu_{n_{\lambda_b}}\delta_{3k}^{r2}\\
C_{r_1}&=2\nu_{n_{\rho_a}}\alpha_{3k}^{r}\beta_{3k}^{r}+2\nu_{n_{\lambda_a}}\gamma_{3k}^{r}\delta_{3k}^{r}+2\nu_{n_{\rho_b}}\alpha_{3k}^{r}\beta_{3k}^{r}+2\nu_{n_{\lambda_b}}\gamma_{3k}^{r}\delta_{3}^{r}
\end{aligned}
\tag{51}
$$

$$
\alpha_{r_k}=\Big(A_{r_k}-\frac{C_{r_k}^2}{4B_{r_k}}\Big),
\tag{52}
$$

$$
\mathbf{D}_1=\mathbf{D}_{l_{\rho_a}m_{l_{\rho_a}},k_a},\quad \mathbf{D}_2=\mathbf{D}_{l_{\lambda_a}m_{l_{\lambda_a}},K_a},\quad \mathbf{D}_3=\mathbf{D}_{l_{\rho_b}m_{l_{\rho_b}},k_b},\quad \mathbf{D}_4=\mathbf{D}_{l_{\lambda_b}m_{l_{\lambda_b}},K_b}
\tag{53}
$$

$$
\tilde g_{ij}=\frac{C_{r_k}^2}{2B_{r_k}^2}c_ic_j+2d_id_j-\frac{C_{r_k}}{B_{r_k}}(c_id_j+c_jd_i),\quad \hat g_{ij}=\frac{1}{2B_{r_k}}c_ic_j
\tag{54}
$$

$$
\begin{aligned}
c_1&=2\nu_{n_{\rho_a}}\beta_{3k}^r,\quad c_2=2\nu_{n_{\lambda_a}}\delta_{3k}^r,\quad c_3=2\nu_{n_{\rho_b}}\beta_{3k}^r,\quad c_4=2\nu_{n_{\lambda_b}}\delta_{3k}^r,\\
d_1&=2\nu_{n_{\rho_a}}\alpha_{3k}^r,\quad d_2=2\nu_{n_{\lambda_a}}\gamma_{3k}^r,\quad d_3=2\nu_{n_{\rho_b}}\alpha_{3k}^r,\quad d_4=2\nu_{n_{\lambda_b}}\gamma_{3k}^r
\end{aligned}
\tag{55}
$$

$$
L_{sum}=\frac{l_{\rho_a}+l_{\lambda_a}+l_{\rho_b}+l_{\lambda_b}}{2}
\tag{56}
$$

$$
\begin{aligned}
&\langle[\phi_{n_{\rho_a}l_{\rho_a}m_{l_{\rho_a}}}(\boldsymbol{r}_{\rho_3})\phi_{n_{\lambda_a}l_{\lambda_a}m_{l_{\lambda_a}}}(\boldsymbol{r}_{\lambda_3})]_{Lm_L}|\widetilde{G}(\boldsymbol{r}_{\rho_3})|[\phi_{n_{\rho_b}l_{\rho_b}m_{l_{\rho_b}}}(\boldsymbol{r}_{\rho_3})\phi_{n_{\lambda_b}l_{\lambda_b}m_{l_{\lambda_b}}}(\boldsymbol{r}_{\lambda_3})]_{Lm_L}\rangle \\
&= N_{n_{\rho_a}l_{\rho_a}}N_{n_{\lambda_a}l_{\lambda_a}}N_{n_{\rho_b}l_{\rho_b}}N_{n_{\lambda_b}l_{\lambda_b}}\frac{1}{(\nu_{n_{\rho_a}})^{l_{\rho_a}}(\nu_{n_{\lambda_a}})^{l_{\lambda_a}}(\nu_{n_{\rho_b}})^{l_{\rho_b}}(\nu_{n_{\lambda_b}})^{l_{\lambda_b}}} \\
&\times \sum_{m_{l_{\rho_a}}m_{l_{\lambda_a}}}(l_{\rho_a}m_{l_{\rho_a}}l_{\lambda_a}m_{l_{\lambda_a}}|Lm_L)\sum_{m_{l_{\rho_b}}m_{l_{\lambda_b}}}(l_{\rho_b}m_{l_{\rho_b}}l_{\lambda_b}m_{l_{\lambda_b}}|Lm_L) \\
&\times 4\pi\Big(\frac{\pi}{B_{r_3}}\Big)^{\frac{3}{2}}\sum_{k_aK_ak_bK_b}C_{l_{\rho_a}m_{l_{\rho_a}}k_a}C_{l_{\lambda_a}m_{l_{\lambda_a}}K_a}C_{l_{\rho_b}m_{l_{\rho_b}}k_b}C_{l_{\lambda_b}m_{l_{\lambda_b}}K_b} \\
&\times \frac{1}{(2l_{\rho_a}+1)!}\int_0^\infty V(r_{\rho_3})Exp(-A_{r_3}r_{\rho_3}^2)r_{\rho_3}^{2l_{\rho_a}+2}dr_{\rho_3}\frac{\hat{g}_{24}^{l_{\lambda_a}}\tilde{g}_{13}^{l_{\rho_a}}}{l_{\lambda_a}!}(\mathbf{D}_1\cdot\mathbf{D}_3)^{l_{\rho_a}}(\mathbf{D}_2\cdot\mathbf{D}_4)^{l_{\lambda_a}}
\end{aligned} \tag{57}
$$

$$
\begin{aligned}
A_{r_3} &= \nu_{n_{\rho_a}} + \nu_{n_{\rho_b}} \\
B_{r_3} &= \nu_{n_{\lambda_a}} + \nu_{n_{\lambda_b}}
\end{aligned} \tag{58}
$$

$$
\tilde{g}_{13} = 2d_1d_3, \quad \hat{g}_{24} = \frac{1}{2B_{r_3}}\times c_2c_4 \tag{59}
$$

$$
c_2 = 2\nu_{n_{\lambda_a}}, \quad c_4 = 2\nu_{n_{\lambda_b}}, \quad d_1 = 2\nu_{n_{\rho_a}}, \quad d_3 = 2\nu_{n_{\rho_b}}, \tag{60}
$$

B.2 Three-body matrix elements of the kinetic-energy operators

For the kinetic energy terms, it can easily be derived that the momentum of each quark can be expressed by relative momentum in baryon center-of-momentum frame, where $\boldsymbol{p}_1 = \boldsymbol{p}_{\lambda_1}$, $\boldsymbol{p}_2 = \boldsymbol{p}_{\lambda_2}$, $\boldsymbol{p}_3 = \boldsymbol{p}_{\lambda_3}$. Then the calculation of kinetic energy matrix element,

$$
\begin{aligned}
&\langle[\phi_{n_{\rho_a}l_{\rho_a}m_{l_{\rho_a}}}(\boldsymbol{p}_{\rho_3})\phi_{n_{\lambda_a}l_{\lambda_a}m_{l_{\lambda_a}}}(\boldsymbol{p}_{\lambda_3})]_L|\sqrt{\boldsymbol{p}_3^2+m_3^2}|[\phi_{n_{\rho_b}l_{\rho_b}m_{l_{\rho_b}}}(\boldsymbol{p}_{\rho_3})\phi_{n_{\lambda_b}l_{\lambda_b}m_{l_{\lambda_b}}}(\boldsymbol{p}_{\lambda_3})]_L\rangle \\
&= \langle[\phi_{n_{\rho_a}l_{\rho_a}m_{l_{\rho_a}}}(\boldsymbol{p}_{\rho_3})\phi_{n_{\lambda_a}l_{\lambda_a}m_{l_{\lambda_a}}}(\boldsymbol{p}_{\lambda_3})]_L|\sqrt{\boldsymbol{p}_{\lambda_3}^2+m_3^2}|[\phi_{n_{\rho_b}l_{\rho_b}m_{l_{\rho_b}}}(\boldsymbol{p}_{\rho_3})\phi_{n_{\lambda_b}l_{\lambda_b}m_{l_{\lambda_b}}}(\boldsymbol{p}_{\lambda_3})]_L\rangle
\end{aligned} \tag{61}
$$

is straightforward. For the kinetic energy terms $\sqrt{\boldsymbol{p}_k^2+m_k^2}_{k=1,2}$, their matrix elements can be described as,

$$
\langle[\phi_{n_{\rho_a}l_{\rho_a}m_{l_{\rho_a}}}(\boldsymbol{p}_{\rho_3})\phi_{n_{\lambda_a}l_{\lambda_a}m_{l_{\lambda_a}}}(\boldsymbol{p}_{\lambda_3})]_L|\sqrt{\boldsymbol{p}_{\lambda_k}^2+m_k^2}|[\phi_{n_{\rho_b}l_{\rho_b}m_{l_{\rho_b}}}(\boldsymbol{p}_{\rho_3})\phi_{n_{\lambda_b}l_{\lambda_b}m_{l_{\lambda_b}}}(\boldsymbol{p}_{\lambda_3})]_L\rangle_{k=1,2} \tag{62}
$$

By performing the Jacobi momentum transformations, $(\boldsymbol{p}_{\rho_3},\boldsymbol{p}_{\lambda_3})\rightarrow(\boldsymbol{p}_{\rho_k},\boldsymbol{p}_{\lambda_k})_{k=1,2}$ over the basis function in momentum representation, we can carry out the calculations about the matrix elements of

Eq.(62). And the expression of kinetic energy matrix elements are explicitly described as,

$$
\begin{aligned}
&\langle[\phi_{n_{\rho_a}l_{\rho_a}m_{l_{\rho_a}}}(\boldsymbol{p}_{\rho_3})\phi_{n_{\lambda_a}l_{\lambda_a}m_{l_{\lambda_a}}}(\boldsymbol{p}_{\lambda_3})]_{Lm_L}|\sqrt{\boldsymbol{p}_{\lambda_k}^2+m_k^2}|[\phi_{n_{\rho_b}l_{\rho_b}m_{l_{\rho_b}}}(\boldsymbol{p}_{\rho_3})\phi_{n_{\lambda_b}l_{\lambda_b}m_{l_{\lambda_b}}}(\boldsymbol{p}_{\lambda_3})]_{Lm_L}\rangle_{k=1,2} \\
&= N_{n_{\rho_a}l_{\rho_a}}N_{n_{\lambda_a}l_{\lambda_a}}N_{n_{\rho_b}l_{\rho_b}}N_{n_{\lambda_b}l_{\lambda_b}}(4\nu_{n_{\rho_a}})^{l_{\rho_a}}(4\nu_{n_{\lambda_a}})^{l_{\lambda_a}}(4\nu_{n_{\rho_b}})^{l_{\rho_b}}(4\nu_{n_{\lambda_b}})^{l_{\lambda_b}}4\pi\left(\frac{\pi}{A_{p_k}}\right)^{\frac{3}{2}} \\
&\times \sum_{m_{l_{\rho_a}}m_{l_{\lambda_a}}}(l_{\rho_a}m_{l_{\rho_a}}l_{\lambda_a}m_{l_{\lambda_a}}|Lm_L)\sum_{m_{l_{\rho_b}}m_{l_{\lambda_b}}}(l_{\rho_b}m_{l_{\rho_b}}l_{\lambda_b}m_{l_{\lambda_b}}|Lm_L) \\
&\times \sum_{m=0}^{Lsum}\frac{m!}{(2m+1)!}\int_0^\infty\sqrt{p_{\lambda_k}^2+m_k^2}Exp(-\alpha_{p_k}p_{\lambda_k}^2)p_{\lambda_k}^{2m+2}dp_{\lambda_k} \\
&\times \sum_{k_aK_ak_bK_b}C_{l_{\rho_a}m_{l_{\rho_a}}k_a}C_{l_{\lambda_a}m_{l_{\lambda_a}}K_a}C_{l_{\rho_b}m_{l_{\rho_b}}k_b}C_{l_{\lambda_b}m_{l_{\lambda_b}}K_b} \qquad (63) \\
&\times \sum_{n_{12}=0}^{Lsum-m}\sum_{n_{13}=0}^{Lsum-m}\sum_{n_{14}=0}^{Lsum-m}\sum_{n_{23}=0}^{Lsum-m}\sum_{n_{24}=0}^{Lsum-m}\sum_{n_{34}=0}^{Lsum-m}\sum_{m_{12}=0}^{m}\sum_{m_{13}=0}^{m}\sum_{m_{14}=0}^{m}\sum_{m_{23}=0}^{m}\sum_{m_{24}=0}^{m}\sum_{m_{34}=0}^{m} \\
&\times \frac{\tilde{g}_{12}^{m_{12}}\tilde{g}_{13}^{m_{13}}\tilde{g}_{14}^{m_{14}}\tilde{g}_{23}^{m_{23}}\tilde{g}_{24}^{m_{24}}\tilde{g}_{34}^{m_3}\hat{g}_{12}^{n_{12}}\hat{g}_{13}^{n_{13}}\hat{g}_{14}^{n_{14}}\hat{g}_{23}^{n_{23}}\hat{g}_{24}^{n_{24}}\hat{g}_{34}^{n_{34}}}{n_{12}!n_{13}!n_{14}!n_{23}!n_{24}!n_{34}!m_{12}!m_{13}!m_{14}!m_{23}!m_{24}!m_{34}!} \\
&\times (\mathbf{D}_1\cdot\mathbf{D}_2)^{n_{12}+m_{12}}(\mathbf{D}_1\cdot\mathbf{D}_3)^{n_{13}+m_{13}}(\mathbf{D}_1\cdot\mathbf{D}_4)^{n_{14}+m_{14}} \\
&\times (\mathbf{D}_2\cdot\mathbf{D}_3)^{n_{23}+m_{23}}(\mathbf{D}_2\cdot\mathbf{D}_4)^{n_{24}+m_{24}}(\mathbf{D}_3\cdot\mathbf{D}_4)^{n_{34}+m_{34}} \\
&\times \delta(n_{12}+n_{13}+n_{14}+n_{23}+n_{24}+n_{34}-(Lsum-m))\delta(m_{12}+m_{13}+m_{14}+m_{23}+m_{24}+m_{34}-m) \\
&\times \delta(n_{12}+n_{13}+n_{14}+m_{12}+m_{13}+m_{14}-l_{\rho_a})\delta(n_{12}+n_{23}+n_{24}+m_{12}+m_{23}+m_{24}-l_{\lambda_a}) \\
&\times \delta(n_{13}+n_{23}+n_{34}+m_{13}+m_{23}+m_{34}-l_{\rho_b})\delta(n_{14}+n_{24}+n_{34}+m_{14}+m_{24}+m_{34}-l_{\lambda_b}) \qquad (64)
\end{aligned}
$$

$$
\alpha_{p_k} = \left(B_{p_k}-\frac{C_{p_k}^2}{4A_{p_k}}\right), \qquad (65)
$$

$$
\begin{aligned}
A_{p_k} &= \frac{\alpha_{3k}^{p2}}{4\nu_{n_{\rho_a}}}+\frac{\gamma_{3k}^{p2}}{4\nu_{n_{\lambda_a}}}+\frac{\alpha_{3k}^{p2}}{4\nu_{n_{\rho_b}}}+\frac{\gamma_{3k}^{p2}}{4\nu_{n_{\lambda_b}}} \\
B_{p_k} &= \frac{\beta_{3k}^{p2}}{4\nu_{n_{\rho_a}}}+\frac{\delta_{3k}^{p2}}{4\nu_{n_{\lambda_a}}}+\frac{\beta_{3k}^{p2}}{4\nu_{n_{\rho_b}}}+\frac{\delta_{3k}^{p2}}{4\nu_{n_{\lambda_b}}} \qquad (66) \\
C_{p_k} &= \frac{\alpha_{3k}^{p}\beta_{3k}^{p}}{2\nu_{n_{\rho_a}}}+\frac{\gamma_{3k}^{p}\delta_{3k}^{p}}{2\nu_{n_{\lambda_a}}}+\frac{\alpha_{3k}^{p}\beta_{3k}^{p}}{2\nu_{n_{\rho_b}}}+\frac{\gamma_{3k}^{p}\delta_{3k}^{p}}{2\nu_{n_{\lambda_b}}}
\end{aligned}
$$

$$
\tilde{g}_{ij} = \frac{C_{p_k}^2}{2B_{p_k}^2}d_id_j+2c_ic_j-\frac{C_{p_k}}{B_{p_k}}(c_id_j+c_jd_i), \quad \hat{g}_{ij} = \frac{1}{2A_{p_k}}d_id_j \qquad (67)
$$

$$
\begin{aligned}
c_1 &= \frac{\beta_{3k}^p}{2\nu_{n_{\rho_a}}}, c_2 = \frac{\delta_{3k}^p}{2\nu_{n_{\lambda_a}}}, c_3 = \frac{\beta_{3k}^p}{2\nu_{n_{\rho_b}}}, c_4 = \frac{\delta_{3k}^p}{2\nu_{n_{\lambda_b}}}, \\
d_1 &= \frac{\alpha_{3k}^p}{2\nu_{n_{\rho_a}}}, d_2 = \frac{\gamma_{3k}^p}{2\nu_{n_{\lambda_a}}}, d_3 = \frac{\alpha_{3k}^p}{2\nu_{n_{\rho_b}}}, d_4 = \frac{\gamma_{3k}^p}{2\nu_{n_{\lambda_b}}} \qquad (68)
\end{aligned}
$$

$$
\begin{aligned}
&\langle[\phi_{n_{\rho_a}l_{\rho_a}m_{l_{\rho_a}}}(\boldsymbol{p}_{\rho_3})\phi_{n_{\lambda_a}l_{\lambda_a}m_{l_{\lambda_a}}}(\boldsymbol{p}_{\lambda_3})]_{Lm_L}|\sqrt{\boldsymbol{p}_{\lambda_3}^2+m_3^2}|[\phi_{n_{\rho_b}l_{\rho_b}m_{l_{\rho_b}}}(\boldsymbol{p}_{\rho_3})\phi_{n_{\lambda_b}l_{\lambda_b}m_{l_{\lambda_b}}}(\boldsymbol{p}_{\lambda_3})]_{Lm_L}\rangle\\
&=N_{n_{\rho_a}l_{\rho_a}}N_{n_{\lambda_a}l_{\lambda_a}}N_{n_{\rho_b}l_{\rho_b}}N_{n_{\lambda_b}l_{\lambda_b}}(4\nu_{n_{\rho_a}})^{l_{\rho_a}}(4\nu_{n_{\lambda_a}})^{l_{\lambda_a}}(4\nu_{n_{\rho_b}})^{l_{\rho_b}}(4\nu_{n_{\lambda_b}})^{l_{\lambda_b}}\\
&\times\sum_{m_{l_{\rho_a}}m_{l_{\lambda_a}}}(l_{\rho_a}m_{l_{\rho_a}}l_{\lambda_a}m_{l_{\lambda_a}}|Lm_L)\sum_{m_{l_{\rho_b}}m_{l_{\lambda_b}}}(l_{\rho_b}m_{l_{\rho_b}}l_{\lambda_b}m_{l_{\lambda_b}}|Lm_L)\\
&\times\sum_{k_aK_ak_bK_b}C_{l_{\rho_a}m_{l_{\rho_a}}k_a}C_{l_{\lambda_a}m_{l_{\lambda_a}}K_a}C_{l_{\rho_b}m_{l_{\rho_b}}k_b}C_{l_{\lambda_b}m_{l_{\lambda_b}}K_b}\frac{1}{l_{\rho_a}}(\mathbf{D}_1\cdot\mathbf{D}_3)^{l_{\rho_a}}(\mathbf{D}_2\cdot\mathbf{D}_4)^{l_{\lambda_a}}\\
&\times 4\pi\Big(\frac{\pi}{A_{p_3}}\Big)^{\frac{3}{2}}\frac{\hat{g}_{13}^{l_{\rho_a}}\tilde{g}_{24}^{l_{\lambda_a}}}{(2m+1)!}\int_0^\infty\sqrt{p_{\lambda_3}^2+m_3^2}Exp(-B_{p_3}p_{\lambda_3}^2)p_{\lambda_3}^{2m+2}dp_{\lambda_3}
\end{aligned}
\tag{69}
$$

$$
\begin{aligned}
A_{p_3}&=\frac{1}{4\nu_{n_{\rho_a}}}+\frac{1}{4\nu_{n_{\rho_b}}}\\
B_{p_3}&=\frac{1}{4\nu_{n_{\lambda_a}}}+\frac{1}{4\nu_{n_{\lambda_b}}}
\end{aligned}
\tag{70}
$$

$$
\hat{g}_{13}=\frac{1}{2A}\times d_1d_3,\quad \tilde{g}_{24}=2c_2c_4,
\tag{71}
$$

$$
\begin{aligned}
c_2&=\frac{1}{2\nu_{n_{\lambda_a}}},\quad c_4=\frac{1}{2\nu_{n_{\lambda_b}}},\\
d_1&=\frac{1}{2\nu_{n_{\rho_a}}},\quad d_3=\frac{1}{2\nu_{n_{\rho_b}}}
\end{aligned}
\tag{72}
$$

B.3 Three-body matrix elements of momentum-dependent factors in the potential energy

Another problem we have to deal with is the matrix elements of the momentum-dependent factors in the Hamiltonian which are combined with spatially dependent potentials such as Eqs.18-21. This problem can be overcome by inserting complete sets of Gaussian functions between the two types of operators. Then the matrix element of the momentum-dependent factor can be evaluated just as the calculations of the kinetic energy terms in momentum space, and the position-dependent parts are obtained in the coordinate space.

$$\begin{aligned}
&\langle[\phi_{n_{\rho_a}l_{\rho_a}m_{l_{\rho_a}}}(\boldsymbol{p}_{\rho_3})\phi_{n_{\lambda_a}l_{\lambda_a}m_{l_{\lambda_a}}}(\boldsymbol{p}_{\lambda_3})]_{Lm_L}|F(\boldsymbol{p}_{\rho_k})|[\phi_{n_{\rho_b}l_{\rho_b}m_{l_{\rho_b}}}(\boldsymbol{p}_{\rho_3})\phi_{n_{\lambda_b}l_{\lambda_b}m_{l_{\lambda_b}}}(\boldsymbol{p}_{\lambda_3})]_{Lm_L}\rangle_{k=1,2}\\
&= N_{n_{\rho_a}l_{\rho_a}}N_{n_{\lambda_a}l_{\lambda_a}}N_{n_{\rho_b}l_{\rho_b}}N_{n_{\lambda_b}l_{\lambda_b}}(4\nu_{n_{\rho_a}})^{l_{\rho_a}}(4\nu_{n_{\lambda_a}})^{l_{\lambda_a}}(4\nu_{n_{\rho_b}})^{l_{\rho_b}}(4\nu_{n_{\lambda_b}})^{l_{\lambda_b}}4\pi\left(\frac{\pi}{B_{p_1}}\right)^{\frac{3}{2}}\\
&\times\sum_{m_{l_{\rho_a}}m_{l_{\lambda_a}}}(l_{\rho_a}m_{l_{\rho_a}}l_{\lambda_a}m_{l_{\lambda_a}}|Lm_L)\sum_{m_{l_{\rho_b}}m_{l_{\lambda_b}}}(l_{\rho_b}m_{l_{\rho_b}}l_{\lambda_b}m_{l_{\lambda_b}}|Lm_L)\\
&\times\sum_{m=0}^{Lsum}\frac{m!}{(2m+1)!}\int_0^\infty F(p_{\rho_k})Exp(-\alpha'_{p_k}p_{\rho_k}^2)p_{\rho_k}^{2m+2}dp_{\rho_k}\\
&\times\sum_{k_aK_ak_bK_b}C_{l_{\rho_a}m_{l_{\rho_a}}k_a}C_{l_{\lambda_a}m_{l_{\lambda_a}}K_a}C_{l_{\rho_b}m_{l_{\rho_b}}k_b}C_{l_{\lambda_b}m_{l_{\lambda_b}}K_b} \qquad (73)\\
&\times\sum_{n_{12}=0}^{Lsum-m}\sum_{n_{13}=0}^{Lsum-m}\sum_{n_{14}=0}^{Lsum-m}\sum_{n_{23}=0}^{Lsum-m}\sum_{n_{24}=0}^{Lsum-m}\sum_{n_{34}=0}^{Lsum-m}\sum_{m_{12}=0}^{m}\sum_{m_{13}=0}^{m}\sum_{m_{14}=0}^{m}\sum_{m_{23}=0}^{m}\sum_{m_{24}=0}^{m}\sum_{m_{34}=0}^{m}\\
&\times\frac{\tilde{g}_{12}^{m_{12}}\tilde{g}_{13}^{m_{13}}\tilde{g}_{14}^{m_{14}}\tilde{g}_{23}^{m_{23}}\tilde{g}_{24}^{m_{24}}\tilde{g}_{34}^{m_3}\hat{g}_{12}^{n_{12}}\hat{g}_{13}^{n_{13}}\hat{g}_{14}^{n_{14}}\hat{g}_{23}^{n_{23}}\hat{g}_{24}^{n_{24}}\hat{g}_{34}^{n_{34}}}{n_{12}!n_{13}!n_{14}!n_{23}!n_{24}!n_{34}!m_{12}!m_{13}!m_{14}!m_{23}!m_{24}!m_{34}!}\\
&\times(\mathbf{D}_1\cdot\mathbf{D}_2)^{n_{12}+m_{12}}(\mathbf{D}_1\cdot\mathbf{D}_3)^{n_{13}+m_{13}}(\mathbf{D}_1\cdot\mathbf{D}_4)^{n_{14}+m_{14}}\\
&\times(\mathbf{D}_2\cdot\mathbf{D}_3)^{n_{23}+m_{23}}(\mathbf{D}_2\cdot\mathbf{D}_4)^{n_{24}+m_{24}}(\mathbf{D}_3\cdot\mathbf{D}_4)^{n_{34}+m_{34}}\\
&\times\delta(n_{12}+n_{13}+n_{14}+n_{23}+n_{24}+n_{34}-(Lsum-m))\delta(m_{12}+m_{13}+m_{14}+m_{23}+m_{24}+m_{34}-m)\\
&\times\delta(n_{12}+n_{13}+n_{14}+m_{12}+m_{13}+m_{14}-l_{\rho_a})\delta(n_{12}+n_{23}+n_{24}+m_{12}+m_{23}+m_{24}-l_{\lambda_a})\\
&\times\delta(n_{13}+n_{23}+n_{34}+m_{13}+m_{23}+m_{34}-l_{\rho_b})\delta(n_{14}+n_{24}+n_{34}+m_{14}+m_{24}+m_{34}-l_{\lambda_b})
\end{aligned}$$

$$F(\boldsymbol{p}_{\rho_k})=\sqrt{\beta(\boldsymbol{p}_{\rho_k})}\quad\textbf{or}\quad F(\boldsymbol{p}_{\rho_k})=\sqrt{\delta(\boldsymbol{p}_{\rho_k})} \qquad (74)$$

$$\begin{aligned}
\beta(\boldsymbol{p}_{\rho_k})&=1+\frac{\boldsymbol{p}_{\rho_k}^2}{\sqrt{\boldsymbol{p}_{\rho_k}^2+m_l^2}\sqrt{\boldsymbol{p}_{\rho_k}^2+m_n^2}}\\
\delta(\boldsymbol{p}_{\rho_k})&=\frac{m_lm_n}{\sqrt{\boldsymbol{p}_{\rho_k}^2+m_l^2}\sqrt{\boldsymbol{p}_{\rho_k}^2+m_n^2}}
\end{aligned} \qquad (75)$$

$$(k,l,n)=(1,2,3),\quad(2,1,3)\quad\textbf{and}\quad(3,2,1)$$

$$\alpha'_{p_k}=\Big(A_{p_k}-\frac{C_{p_k}^2}{4B_{p_k}}\Big), \qquad (76)$$

$$\tilde{g}_{ij}=\frac{C_{p_k}^2}{2B_{p_k}^2}c_ic_j+2d_id_j-\frac{C_{p_k}}{B_{p_k}}(c_id_j+c_jd_i),\quad\hat{g}_{ij}=\frac{1}{2B_{p_k}}c_ic_j \qquad (77)$$

$$
\begin{aligned}
&\langle[\phi_{n_{\rho_a} l_{\rho_a} m_{l_{\rho_a}}}(\boldsymbol{p}_{\rho_3})\phi_{n_{\lambda_a} l_{\lambda_a} m_{l_{\lambda_a}}}(\boldsymbol{p}_{\lambda_3})]_{Lm_L}|F(p_{\rho_3})|[\phi_{n_{\rho_b} l_{\rho_b} m_{l_{\rho_b}}}(\boldsymbol{p}_{\rho_3})\phi_{n_{\lambda_b} l_{\lambda_b} m_{l_{\lambda_b}}}(\boldsymbol{p}_{\lambda_3})]_{Lm_L}\rangle \\
&= N_{n_{\rho_a} l_{\rho_a}} N_{n_{\lambda_a} l_{\lambda_a}} N_{n_{\rho_b} l_{\rho_b}} N_{n_{\lambda_b} l_{\lambda_b}} (4\nu_{n_{\rho_a}})^{l_{\rho_a}} (4\nu_{n_{\lambda_a}})^{l_{\lambda_a}} (4\nu_{n_{\rho_b}})^{l_{\rho_b}} (4\nu_{n_{\lambda_b}})^{l_{\lambda_b}} \\
&\times \sum_{m_{l_{\rho_a}} m_{l_{\lambda_a}}} (l_{\rho_a} m_{l_{\rho_a}} l_{\lambda_a} m_{l_{\lambda_a}}|Lm_L) \sum_{m_{l_{\rho_b}} m_{l_{\lambda_b}}} (l_{\rho_b} m_{l_{\rho_b}} l_{\lambda_b} m_{l_{\lambda_b}}|Lm_L) \\
&\times \sum_{k_a K_a k_b K_b} C_{l_{\rho_a} m_{l_{\rho_a}} k_a} C_{l_{\lambda_a} m_{l_{\lambda_a}} K_a} C_{l_{\rho_b} m_{l_{\rho_b}} k_b} C_{l_{\lambda_b} m_{l_{\lambda_b}} K_b} \frac{1}{l_{\lambda_a !}} (\mathbf{D}_1 \cdot \mathbf{D}_3)^{l_{\rho_a}} (\mathbf{D}_2 \cdot \mathbf{D}_4)^{l_{\lambda_a}} \\
&\times 4\pi \big(\frac{\pi}{B_{p_3}}\big)^{\frac{3}{2}} \frac{\tilde{g}_{13}^{l_{\rho_a}} \hat{g}_{24}^{l_{\lambda_a}}}{(2l\rho_a+1)!} \int_0^\infty F(p_{\rho_3}) Exp(-A_{p_3} p_{\rho_3}^2) p_{\rho_3}^{2m+2} dp_{\rho_3}
\end{aligned}
$$

$$
\begin{aligned}
&\tilde{g}_{13} = 2d_1 d_3, \quad \hat{g}_{24} = \frac{1}{2B_{p3}} c_2 c_4, \\
&c_2 = \frac{1}{2\nu_{n_{\lambda_a}}}, c_4 = \frac{1}{2\nu_{n_{\lambda_b}}}, d_1 = \frac{1}{2\nu_{n_{\rho_a}}}, d_3 = \frac{1}{2\nu_{n_{\rho_b}}},
\end{aligned} \tag{78}
$$

B.4 Three-body matrix elements of the potential energy with spin−orbit interactions

As for the color matrix element, the matrix elements of spin-spin and spin-orbit terms, they can easily be obtained by using the results of potential energy matrix elements. The explicit structures of the spin-orbit matrix elements are illustrated as,

$$
\begin{aligned}
&\langle[\phi_{n_{\rho_a} l_{\rho_a} m_{l_{\rho_a}}}(\boldsymbol{r}_{\rho_3})\phi_{n_{\lambda_a} l_{\lambda_a} m_{l_{\lambda_a}}}(\boldsymbol{r}_{\lambda_3})]_{Lm_L}[\chi_{s'_1 m_{s'_1}} \chi_{s'_2 m_{s'_2}}]_{sm_s}|\widetilde{G}(r_{\rho_3})\mathbf{s}_i \cdot \boldsymbol{l}_\rho| \\
&[\phi_{n_{\rho_b} l_{\rho_b} m_{l_{\rho_b}}}(\boldsymbol{r}_{\rho_3})\phi_{n_{\lambda_b} l_{\lambda_b} m_{l_{\lambda_b}}}(\boldsymbol{r}_{\lambda_3})]_{Lm_L}[\chi_{s_1 m_{s_1}} \chi_{s_2 m_{s_2}}]_{sm_s}\rangle_{i=1,2} \\
&= \sum_{m_{s_1}=-1/2}^{1/2} \sum_{m_{s'_1}=-1/2}^{1/2} \sum_{m_{l_{\rho_a}}=-l_{\rho_a}}^{l_{\rho_a}} \sum_{m_{l_{\rho_b}}=-l_{\rho_b}}^{l_{\rho_b}} (l_{\rho_a} m_{l_{\rho_a}} l_{\lambda_a} m_{l_{\lambda_a}}|Lm_L)(l_{\rho_b} m_{l_{\rho_b}} l_{\lambda_b} m_{l_{\lambda_b}}|Lm_L) \\
&\times (s'_1 m_{s'_1} s'_2 m_{s'_2}|sm_s)(s_1 m_{s_1} s_2 m_{s_2}|sm_s) \times \\
&\Big[\langle\phi_{n_{\rho_a} l_{\rho_a} m_{l_{\rho_a}}}(\boldsymbol{r}_{\rho_3})\phi_{n_{\lambda_a} l_{\lambda_a} m_{l_{\lambda_a}}}(\boldsymbol{r}_{\lambda_3})|\widetilde{G}(r_{\rho_3})|\phi_{n_{\rho_b} l_{\rho_b} m_{l_{\rho_b}}+1}(\boldsymbol{r}_{\rho_3})\phi_{n_{\lambda_b} l_{\lambda_b} m_{l_{\lambda_b}}}(\boldsymbol{r}_{\lambda_3})\rangle \\
&\times \frac{1}{2}\sqrt{(l_{\rho_b} - m_{l_{\rho_b}})(l_{\rho_b} + m_{l_{\rho_b}} + 1)}\sqrt{(s_i + m_{s_i})(s_i - m_{s_i} + 1)}\delta_{s'_i s_i}\delta_{m_{s'_i} m_{s_i} - 1} \\
&+ \langle\phi_{n_{\rho_a} l_{\rho_a} m_{l_{\rho_a}}}(\boldsymbol{r}_{\rho_3})\phi_{n_{\lambda_a} l_{\lambda_a} m_{l_{\lambda_a}}}(\boldsymbol{r}_{\lambda_3})|\widetilde{G}(r_{\rho_3})|\phi_{n_{\rho_b} l_{\rho_b} m_{l_{\rho_b}}-1}(\boldsymbol{r}_{\rho_3})\phi_{n_{\lambda_b} l_{\lambda_b} m_{l_{\lambda_b}}}(\boldsymbol{r}_{\lambda_3})\rangle \\
&\times \frac{1}{2}\sqrt{(l_{\rho_b} + m_{l_{\rho_b}})(l_{\rho_b} - m_{l_{\rho_b}} + 1)}\sqrt{(s_i - m_{s_i})(s_i + m_{s_i} + 1)}\delta_{s'_i s_i}\delta_{m_{s'_i} m_{s_i} + 1} \\
&+ \langle\phi_{n_{\rho_a} l_{\rho_a} m_{l_{\rho_a}}}(\boldsymbol{r}_{\rho_3})\phi_{n_{\lambda_a} l_{\lambda_a} m_{l_{\lambda_a}}}(\boldsymbol{r}_{\lambda_3})|\widetilde{G}(r_{\rho_3})|\phi_{n_{\rho_b} l_{\rho_b} m_{l_{\rho_b}}}(\boldsymbol{r}_{\rho_3})\phi_{n_{\lambda_b} l_{\lambda_b} m_{l_{\lambda_b}}}(\boldsymbol{r}_{\lambda_3})\rangle m_{l_{\rho_b}} m_{s_i} \delta_{m_{s'_i} m_{s_i}}\Big]
\end{aligned} \tag{79}
$$

$$
\begin{aligned}
&\Big\langle \Big[[[\phi_{n_{\rho_a} l_{\rho_a} m_{l_{\rho_a}}}(\boldsymbol{r}_{\rho 3}) \phi_{n_{\lambda_a} l_{\lambda_a} m_{l_{\lambda_a}}}(\boldsymbol{r}_{\lambda 3})]_{Lm_L} [\chi_{s'_1 m_{s'_1}} \chi_{s'_2 m_{s'_2}}]_{sm_s}\Big]_{jm_j} \chi_{s'_3 m_{s'_3}} \Big]_{JM} |\widetilde{G}(r_{\lambda 3}) \mathbf{s}_3 \cdot \boldsymbol{l}_\lambda| \\
&\Big[[[\phi_{n_{\rho_b} l_{\rho_b} m_{l_{\rho_b}}}(\boldsymbol{r}_{\rho 3}) \phi_{n_{\lambda_b} l_{\lambda_b} m_{l_{\lambda_b}}}(\boldsymbol{r}_{\lambda 3})]_{Lm_L} [\chi_{s_1 m_{s_1}} \chi_{s_2 m_{s_2}}]_{sm_s}\Big]_{jm_j} \chi_{s_3 m_{s_3}} \Big]_{JM} \Big\rangle \\
&= \sum_{m_{s_3}=-1/2}^{1/2} \sum_{m_{s'_3}=-1/2}^{1/2} \sum_{m_{l_{\rho_a}}=-l_{\rho_a}}^{l_{\rho_a}} \sum_{m_{l_{\rho_b}}=-l_{\rho_b}}^{l_{\rho_b}} \sum_{m_s=-s}^{s} \sum_{m_{s'}=-s'}^{s'} (l_{\rho_a} m_{l_{\rho_a}} l_{\lambda_a} m_{l_{\lambda_a}} | L m_L) \\
&\times (l_{\rho_b} m_{l_{\rho_b}} l_{\lambda_b} m_{l_{\lambda_b}} | L m_L)(s' m_{s'} L m_L | j m_j)(s m_s L m_L | j m_j)(j m_j s'_3 m_{s'_3} | JM)(j m_j s_3 m_{s_3} | JM) \\
&\times \Big[\langle \phi_{n_{\rho_a} l_{\rho_a} m_{l_{\rho_a}}}(\boldsymbol{r}_{\rho 3}) \phi_{n_{\lambda_a} l_{\lambda_a} m_{l_{\lambda_a}}}(\boldsymbol{r}_{\lambda 3}) | \widetilde{G}(r_{\lambda 3}) | \phi_{n_{\rho_b} l_{\rho_b} m_{l_{\rho_b}}}(\boldsymbol{r}_{\rho 3}) \phi_{n_{\lambda_b} l_{\lambda_b} m_{l_{\lambda_b}}+1}(\boldsymbol{r}_{\lambda 3}) \rangle \\
&\times \frac{1}{2} \sqrt{(l_{\lambda_b} - m_{l_{\lambda_b}})(l_{\lambda_b} + m_{l_{\lambda_b}} + 1)} \sqrt{(s_3 + m_{s_3})(s_3 - m_{s_3} + 1)} \delta_{m_{s'_3} m_{s_3} - 1} \\
&+ \langle \phi_{n_{\rho_a} l_{\rho_a} m_{l_{\rho_a}}}(\boldsymbol{r}_{\rho 3}) \phi_{n_{\lambda_a} l_{\lambda_a} m_{l_{\lambda_a}}}(\boldsymbol{r}_{\lambda 3}) | \widetilde{G}(r_{\lambda 3}) | \phi_{n_{\rho_b} l_{\rho_b} m_{l_{\rho_b}}}(\boldsymbol{r}_{\rho 3}) \phi_{n_{\lambda_b} l_{\lambda_b} m_{l_{\lambda_b}}-1}(\boldsymbol{r}_{\lambda 3}) \rangle \\
&\times \frac{1}{2} \sqrt{(l_{\lambda_b} + m_{l_{\lambda_b}})(l_{\lambda_b} - m_{l_{\lambda_b}} + 1)} \sqrt{(s_3 - m_{s_3})(s_i + m_{s_3} + 1)} \delta_{m_{s'_3} m_{s_3} + 1} \\
&+ \langle \phi_{n_{\rho_a} l_{\rho_a} m_{l_{\rho_a}}}(\boldsymbol{r}_{\rho 3}) \phi_{n_{\lambda_a} l_{\lambda_a} m_{l_{\lambda_a}}}(\boldsymbol{r}_{\lambda 3}) | \widetilde{G}(r_{\lambda 3}) | \phi_{n_{\rho_b} l_{\rho_b} m_{l_{\rho_b}}}(\boldsymbol{r}_{\rho 3}) \phi_{n_{\lambda_b} l_{\lambda_b} m_{l_{\lambda_b}}}(\boldsymbol{r}_{\lambda 3}) \rangle m_{l_{\lambda_b}} m_{s_3} \delta_{m_{s'_3} m_{s_3}} \Big]
\end{aligned} \tag{80}
$$

$$
\begin{aligned}
&\langle [\phi_{n_{\rho_a} l_{\rho_a} m_{l_{\rho_a}}}(\boldsymbol{r}_{\rho 3}) \phi_{n_{\lambda_a} l_{\lambda_a} m_{l_{\lambda_a}}}(\boldsymbol{r}_{\lambda 3})]_{Lm_L} | \widetilde{G}(r_{\lambda 3}) | [\phi_{n_{\rho_b} l_{\rho_b} m_{l_{\rho_b}}}(\boldsymbol{r}_{\rho 3}) \phi_{n_{\lambda_b} l_{\lambda_b} m_{l_{\lambda_b}}}(\boldsymbol{r}_{\lambda 3})]_{Lm_L} \rangle \\
&= N_{n_{\rho_a} l_{\rho_a}} N_{n_{\lambda_a} l_{\lambda_a}} N_{n_{\rho_b} l_{\rho_b}} N_{n_{\lambda_b} l_{\lambda_b}} \frac{1}{(\nu_{n_{\rho_a}})^{l_{\rho_a}} (\nu_{n_{\lambda_a}})^{l_{\lambda_a}} (\nu_{n_{\rho_b}})^{l_{\rho_b}} (\nu_{n_{\lambda_b}})^{l_{\lambda_b}}} \\
&\times \sum_{m_{l_{\rho_a}} m_{l_{\lambda_a}}} (l_{\rho_a} m_{l_{\rho_a}} l_{\lambda_a} m_{l_{\lambda_a}} | L m_L) \sum_{m_{l_{\rho_b}} m_{l_{\lambda_b}}} (l_{\rho_b} m_{l_{\rho_b}} l_{\lambda_b} m_{l_{\lambda_b}} | L m_L) \\
&\times 4\pi \Big(\frac{\pi}{A_{r_3}}\Big)^{\frac{3}{2}} \sum_{k_a K_a k_b K_b} C_{l_{\rho_a} m_{l_{\rho_a}} k_a} C_{l_{\lambda_a} m_{l_{\lambda_a}} K_a} C_{l_{\rho_b} m_{l_{\rho_b}} k_b} C_{l_{\lambda_b} m_{l_{\lambda_b}} K_b} \\
&\times \frac{1}{(2m+1)!} \int_0^\infty V(r_{\lambda 3}) Exp(-B_{r_3} r_{\lambda 3}^2) r_{\lambda 3}^{2m+2} dr_{\lambda 3} \frac{\tilde{g}_{24}^{l_{\lambda_a}} \hat{g}_{13}^{l_{\rho_a}}}{l_{\rho_a}!} (\mathbf{D}_1 \cdot \mathbf{D}_3)^{l_{\rho_a}} (\mathbf{D}_2 \cdot \mathbf{D}_4)^{l_{\lambda_a}}
\end{aligned} \tag{81}
$$

$$
\tilde{g}_{24} = 2c_2 c_4, \quad \hat{g}_{13} = \frac{1}{2A_{r_3}} d_1 d_3 \tag{82}
$$

$$
c_2 = 2\nu_{n_{\lambda_a}}, \quad c_4 = 2\nu_{n_{\lambda_b}}, \quad d_1 = 2\nu_{n_{\rho_a}}, \quad d_3 = 2\nu_{n_{\rho_b}}, \tag{83}
$$

A.5 Relations used in matrix elements of the tensor term

Finally, it only remains to discuss how we deal with the tensor term in Hamiltonian. We first evaluate the matrix element of the tensor term in spin space,

$$\langle\chi_{s41}|\mathbf{S}_1\cdot\hat{\mathbf{r}}_\rho\mathbf{S}_2\cdot\hat{\mathbf{r}}_\rho|\chi_{s41}\rangle = \langle\chi_{s44}|\mathbf{S}_1\cdot\hat{\mathbf{r}}_\rho\mathbf{S}_2\cdot\hat{\mathbf{r}}_\rho|\chi_{s44}\rangle = \frac{\mathbf{cos}^2\theta}{4} \tag{84}$$

$$\langle\chi_{s42}|\mathbf{S}_1\cdot\hat{\mathbf{r}}_\rho\mathbf{S}_2\cdot\hat{\mathbf{r}}_\rho|\chi_{s42}\rangle = \langle\chi_{s43}|\mathbf{S}_1\cdot\hat{\mathbf{r}}_\rho\mathbf{S}_2\cdot\hat{\mathbf{r}}_\rho|\chi_{s43}\rangle = \frac{1}{24}(1-3\mathbf{cos}2\theta) \tag{85}$$

$$\langle\chi_{s21}|\mathbf{S}_1\cdot\hat{\mathbf{r}}_\rho\mathbf{S}_2\cdot\hat{\mathbf{r}}_\rho|\chi_{s21}\rangle = \langle\chi_{s22}|\mathbf{S}_1\cdot\hat{\mathbf{r}}_\rho\mathbf{S}_2\cdot\hat{\mathbf{r}}_\rho|\chi_{s22}\rangle = \frac{1}{12} \tag{86}$$

$$\langle\chi_{As21}|\mathbf{S}_1\cdot\hat{\mathbf{r}}_\rho\mathbf{S}_2\cdot\hat{\mathbf{r}}_\rho|\chi_{As21}\rangle = \langle\chi_{As22}|\mathbf{S}_1\cdot\hat{\mathbf{r}}_\rho\mathbf{S}_2\cdot\hat{\mathbf{r}}_\rho|\chi_{As22}\rangle = -\frac{1}{4} \tag{87}$$

where χ_{s41},χ_{s42},χ_{s43},χ_{s44} are the total spin wave functions of a baryon, which are symmetric quadruplet state, χ_{s21}, χ_{s22}, χ_{As21} and χ_{As22} are the mixed symmetric/antisymmetric states. These spin wave functions and a few relations used in deriving Eqs.(84)-(87) are shown as,

$$\begin{aligned}
\chi_{s41} &= \chi_{\frac{1}{2}}\otimes\chi_{\frac{1}{2}}\otimes\chi_{\frac{1}{2}}\\
\chi_{s42} &= \frac{1}{\sqrt{3}}(\chi_{-\frac{1}{2}}\otimes\chi_{\frac{1}{2}}\otimes\chi_{\frac{1}{2}}+\chi_{\frac{1}{2}}\otimes\chi_{-\frac{1}{2}}\otimes\chi_{\frac{1}{2}}+\chi_{\frac{1}{2}}\otimes\chi_{\frac{1}{2}}\otimes\chi_{-\frac{1}{2}})\\
\chi_{s43} &= \frac{1}{\sqrt{3}}(\chi_{-\frac{1}{2}}\otimes\chi_{-\frac{1}{2}}\otimes\chi_{\frac{1}{2}}+\chi_{-\frac{1}{2}}\otimes\chi_{\frac{1}{2}}\otimes\chi_{-\frac{1}{2}}+\chi_{\frac{1}{2}}\otimes\chi_{-\frac{1}{2}}\otimes\chi_{-\frac{1}{2}})\\
\chi_{s44} &= \chi_{-\frac{1}{2}}\otimes\chi_{-\frac{1}{2}}\otimes\chi_{-\frac{1}{2}}\\
\chi_{s21} &= \frac{1}{\sqrt{6}}(\chi_{\frac{1}{2}}\otimes\chi_{-\frac{1}{2}}\otimes\chi_{\frac{1}{2}}+\chi_{-\frac{1}{2}}\otimes\chi_{\frac{1}{2}}\otimes\chi_{\frac{1}{2}}-2\chi_{\frac{1}{2}}\otimes\chi_{\frac{1}{2}}\otimes\chi_{-\frac{1}{2}})\\
\chi_{s22} &= -\frac{1}{\sqrt{6}}(\chi_{\frac{1}{2}}\otimes\chi_{-\frac{1}{2}}\otimes\chi_{-\frac{1}{2}}+\chi_{-\frac{1}{2}}\otimes\chi_{\frac{1}{2}}\otimes\chi_{-\frac{1}{2}}-2\chi_{-\frac{1}{2}}\otimes\chi_{-\frac{1}{2}}\otimes\chi_{\frac{1}{2}})\\
\chi_{As21} &= \frac{1}{\sqrt{2}}(\chi_{\frac{1}{2}}\otimes\chi_{-\frac{1}{2}}\otimes\chi_{\frac{1}{2}}-\chi_{-\frac{1}{2}}\otimes\chi_{\frac{1}{2}}\otimes\chi_{\frac{1}{2}})\\
\chi_{As22} &= \frac{1}{\sqrt{2}}(\chi_{\frac{1}{2}}\otimes\chi_{-\frac{1}{2}}\otimes\chi_{-\frac{1}{2}}-\chi_{-\frac{1}{2}}\otimes\chi_{\frac{1}{2}}\otimes\chi_{-\frac{1}{2}})
\end{aligned} \tag{88}$$

$$(\mathbf{S}\cdot\hat{\mathbf{r}}_\rho)_1 = \begin{pmatrix} 0 & \frac{1}{2}\mathbf{sin}\theta\mathbf{cos}\phi \\ \frac{1}{2}\mathbf{sin}\theta\mathbf{cos}\phi & 0 \end{pmatrix} \tag{89}$$

$$(\mathbf{S}\cdot\hat{\mathbf{r}}_\rho)_2 = \begin{pmatrix} 0 & -\frac{i}{2}\mathbf{sin}\theta\mathbf{sin}\phi \\ \frac{1}{2}\mathbf{sin}\theta\mathbf{sin}\phi & 0 \end{pmatrix} \tag{90}$$

$$(\mathbf{S}\cdot\hat{\mathbf{r}}_\rho)_3 = \begin{pmatrix} \frac{1}{2}\mathbf{cos}\theta & 0 \\ 0 & \frac{1}{2}\mathbf{cos}\theta \end{pmatrix} \tag{91}$$

$$\mathbf{S}_1\cdot\hat{\mathbf{r}}_\rho\mathbf{S}_2\cdot\hat{\mathbf{r}}_\rho = \sum_{i=1}^{3}\sum_{j=1}^{3}(\mathbf{S}\cdot\hat{\mathbf{r}}_\rho)_i\otimes(\mathbf{S}\cdot\hat{\mathbf{r}}_\rho)_j\otimes I \tag{92}$$

Finally, the remaining angular part in Eqs.(84)-(87) can be integrated together with the spatial part.